



Natural climate change and glaciations

Uwe Walzer^{*}, Roland Hendel

Institut für Geowissenschaften, Friedrich-Schiller-Universität, Humboldtstrasse 11, 07743 Jena, Germany

ARTICLE INFO

Keywords:

Natural climate change
Glaciations
Onsets and terminations
LIPs
Proximity to paleoequator
Bifurcations between stable states

ABSTRACT

We investigated the interactions between continental growth and breakup, inorganic carbonate–silicate cycle, volcanic activity, glaciations, natural climate change, and biotic evolution. As far as volcanism is concerned, the large igneous provinces (LIPs) are proving to be particularly effective. However, this conclusion is not valid without additional assumptions. The effects of the eruptions of LIPs must be seen in connection with the physical climatology at the time of the eruption, the proximity of the LIPs to the paleoequator, the strength of the eruption and the chemical composition of the lava and the emitted gases. The faint young Sun was compensated for by higher atmospheric concentrations of greenhouse gases on the early Earth. These greenhouse gases were subsequently drawdown by climate-dependent silicate weathering as the solar radiation increased. Although some authors have expected, that growth of juvenile continental crust or continental breakup would be followed by a glaciation, this is not always the case. Glaciations have abrupt onsets and terminations, and we examined previously proposed hypotheses to explain glaciations and the abrupt onsets and terminations. The hypothesis that pulses of continental growth or supercontinent breakup events resulted in intensified silicate weathering is essentially correct but does not explain everything. Apparently, the hypothesis refers to an existing mechanism, but there must be other, hitherto hidden influences. Multiple stable states in the climate system are separated by unstable jumps (bifurcations) between stable states. This is primarily a reflection of ice-albedo feedback, particularly between sea ice and sea. Ice-albedo feedback ensures rapid advance and retreat of marine ice margins across the tropics. This explains abrupt onset and termination of snowball Earth periods. We show that hypotheses based on inorganic carbonate–silicate cycle and, to a considerably lesser degree, on biotic factors can explain most natural climate change, but not the abrupt onset and termination of snowball Earth periods. Furthermore, we discuss the temporal distribution of glacials and interglacials within a glaciation. This distribution is controlled mainly by the mechanics of our planetary system, influenced by internal feedback mechanisms of the Earth system. Short-period changes in the weather are caused by changes in the solar magnetic field.

1. Introduction

A much-discussed topic today is man-made climate change. This is explicitly *not* the subject of this paper. However, in order to deal with man-made climate change in a serious way, it is necessary to know what climate change would be happening by nature anyway. We consider natural climate change mainly on the long-term geological scale, i.e. over the 4567 Ma of Earth's existence. Medium-term events such as the division of a glaciation into glacials and interglacials are discussed towards the end of the paper. At the very end, very short-term weather events caused by variations in solar magnetism are discussed. Our motivation comes from a computational model developed by [Walzer and Hendel \(2022\)](#) in which the evolution of the Earth's mantle was studied. The model utilizes the full set of physical balance equations that were

solved for a 3D spherical-shell mantle and for 4567 Ma. The model leads to the correct volume of the present-day continents and the present-day heat flow density, and also the timing of formation of juvenile continental crust. The latter is similar to the global detrital zircon ages presented by [Puetz and Condie \(2019\)](#), [Puetz and Condie \(2022\)](#). In both cases, it appears the continental crust grew *episodically* rather than in a steady state fashion. A question that now arises is whether a strong peak in continental growth followed by silicate weathering produces a marked decrease in ocean and atmospheric temperatures. This matter turned out to be much more complex than assumed at first sight. Quite different mechanisms had to be considered separately. At this point, we would like to state in advance that we are addressing different mechanisms to explain natural climate change. While many authors favor monocausal hypotheses, we have concluded that the superposition of

^{*} Corresponding author at: Institut für Geowissenschaften, Friedrich-Schiller-Universität, Humboldtstrasse 11, 07743 Jena, Germany.
E-mail address: u.walzer@uni-jena.de (U. Walzer).

several mechanisms simultaneously causes natural climate change. Thus, our work is not about refuting one set of proposals after another in order to propose our own all-encompassing hypothesis at the end. Rather, we seek to evaluate the influence of different mechanisms in order to arrive at a balanced judgment.

A particularly interesting phenomenon are the large glaciations, especially snowball Earth periods. Their onsets and terminations turn out to be abrupt. They occur even faster than originally assumed. The cause of this remarkable phenomenon is mainly discussed in the Section 2.3.

2. Natural climate change: slow changes

The inorganic carbonate–silicate cycle is the dominant mechanism for the *slow* natural climate change. It was a long way before this finding could be summarized so succinctly. To anticipate, the abrupt onsets and terminations of the major glaciations are caused by a completely different mechanism.

2.1. Preliminaries: the faint young Sun problem

The chemical composition and physical structure of stars are now well understood (e.g., [Kippenhahn et al., 2013](#)). This knowledge is a direct consequence of a theory of the first type mentioned in Section 2 of [Walzer and Hendel \(2022\)](#). During Earth's early history, the ratio of hydrogen to helium was relatively high in the solar core. Radiation energy was generated by nuclear fusion of hydrogen into helium. The helium production enhanced the density of the solar core, gravitational contraction, and isentropic heating. Therefore, the solar luminosity increased gradually over time. At 4567 Ma, the solar luminosity was only about 70% of the present value ([Bahcall et al., 2001](#)). Therefore, it would be expected that all surface water was frozen during the Hadean and Archean. However, the oceans would probably not freeze to the bottom, but to an equilibrium depth that depends on geothermal flux, diffusivity of the ice, and surface temperature. In addition, it has been established by geological observation that there was liquid water on Earth's surface during the Archean. There are two locations where Paleoproterozoic sediments are well preserved and can be studied to investigate the faint young Sun paradox: the Pilbara region of Australia and the Barberton Greenstone Belt in South Africa. The sedimentary rocks of the Moodies Group in South Africa are approximately 3.22–3.10 Ga in age, and consist of well preserved, shallow-water strata ([Heubeck and Lowe, 1994](#); [Heubeck and Lowe, 1994](#); [Heubeck et al., 2013](#)). These rocks contain evidence of microbial life (e.g., endolithic bacteria). Therefore, there must have been shallow water and sunlight at this time. Liquid water on Earth's surface first appeared at 4.4 Ga ([Valley et al., 2002](#); [Nutman, 2006](#)). There have been several attempts to explain the faint young Sun paradox ([Feulner, 2012](#)). One explanation is that the early atmosphere contained considerably more greenhouse gases than today. [Sagan and Mullen \(1972\)](#) proposed that a high proportion of reduced gases (e.g., ammonia and methane) existed in the early atmosphere. However, ammonia is photochemically unstable. There are also some other counter-arguments. In this context, it should be noted that ammonia and methane may add a greenhouse gas forcing, but they do not explain self-adaptation to increasing solar brightness. Nonetheless, [Ueno et al. \(2009\)](#) revived the ammonia hypothesis and investigated the UV absorption spectra of $^{32}\text{SO}_2$, $^{33}\text{SO}_2$, and $^{34}\text{SO}_2$ in order to interpret the geological record. The increase in atmospheric oxygen during the Great Oxidation Event (GOE) would have diminished the abundances of ammonia and methane, and possibly caused the four glaciations between 2460 and 2240 Ma. Given that the greenhouse effect of NH_3 and CH_4 is much higher than that of CO_2 and H_2O , this appears to be an attractive hypothesis. However, even if we accept the old value of 2400 Ma for the onset of the first Paleoproterozoic ice age ([Kirschvink et al., 2000](#)), then it clearly occurred before the Great Oxidation Event that is dated to 2300 Ma. The first three Paleoproterozoic ice ages occurred at

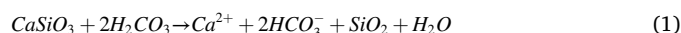
2460–2435 Ma (Ramsay Lake), 2410–2384 Ma (Bruce), and 2340–2310 Ma (Gowganda). - These approximate ages were compiled from [Tang and Chen \(2013\)](#), [Gumsley et al. \(2017\)](#), [Rasmussen et al. \(2013\)](#), [Gaucher and Frei \(2018\)](#), [Caquingue et al. \(2018\)](#), and are used primarily to produce [Figs. 1 through 4](#). An important message from these Figures, however, is that despite the close succession of the four Paleoproterozoic glaciations, an extraordinarily long period follows until the Sturtian glacial onset (717.5 Ma after [Hoffman et al. \(2017\)](#), which is ice-free. This extraordinary phenomenon requires explanation. To anticipate, the suggestions made in this paper in this regard are only tentative, i.e., it is worthwhile to continue thinking about this problem. - Recently, [Luo et al. \(2016\)](#) constrained the timing of the Great Oxidation Event to 2330 Ma. They concluded that oxygenation occurred rapidly, over a period of 1–10 Ma. [Ueno et al. \(2009\)](#) proposed that carbonyl sulfide could shield ammonia from UV radiation. Carbonyl sulfide is stable today because it is not oxidized by OH radicals. However, there was no ozone layer during the Archean. Therefore, carbonyl sulfide would have been decomposed by photolysis ([Domagal-Goldman et al., 2011](#); [Claire et al., 2014](#)). Hence, it can be assumed that ammonia was not an important greenhouse gas on the early Earth.

As suggested by [Feulner \(2012\)](#), carbon dioxide and methane appear to be the best candidates to solve the faint young Sun paradox. Previous studies have estimated the partial pressure of CO_2 during the Archean and early Proterozoic. [Driese et al. \(2011\)](#) obtained 0.003–0.015 bar CO_2 at 2691 Ma, based on a paleosol outcrop in northeastern Minnesota, USA. [Kanzaki and Murakami \(2015\)](#) determined 0.03–0.15 bar CO_2 from the Mt. Roe paleosol (Australia) at 2770 Ma, 0.02–0.75 bar CO_2 from the Bird paleosol (South Africa) at 2750 Ma, and 0.05–0.15 bar CO_2 from the Pronto paleosol (Canada) at 2460 Ga. Determining CH_4 levels in the Archean and Proterozoic atmosphere are challenging. [Claire et al. \(2006\)](#) presented a biochemical box model coupled to photochemistry and proposed a decrease in CH_4 from 2000 μbar CH_4 at 4.0 Ga to 5 μbar CH_4 at 2.5 Ga. [Catling and Zahnle \(2020\)](#) estimated the CH_4 level of the Archean atmosphere to be 10^2 to 10^4 times the present-day value.

2.2. The inorganic carbonate–silicate cycle

2.2.1. General considerations

[Walker et al. \(1981\)](#) proposed that the partial pressure of CO_2 is buffered by a negative feedback mechanism, because the rate of silicate weathering depends on surface temperature, and the surface temperature depends on the partial pressure of CO_2 . Despite the increasing solar luminosity with time, Earth's surface temperature remained relatively constant, but with some considerably large fluctuations, around the mean. The negative feedback stabilizes the long-term climate, where the chemical weathering of Ca silicates can be expressed as follows:



where carbonic acid is produced at low concentrations by the chemical reaction between atmospheric carbon dioxide and rain water. Rivers carry HCO_3^- and Ca^{2+} into the oceans where calcium carbonate is precipitated on the ocean floor as follows:



Similarly, other cations are transported to the ocean floor and the net reactions can be schematically represented as follows:



Most CO_2 is returned to the atmosphere by andesitic volcanoes near subduction zones, but some carbonate is subducted into the mantle. Many studies have assumed that, over geological timescales, this chemical weathering of continental rocks is of key importance in decreasing atmospheric CO_2 . Similarly, [Siever \(1992\)](#) suggested that the

Precambrian carbonate–silicate cycle was dominated by inorganic reactions. He was already aware that the influx of silica to the Neoproterozoic ocean was governed, as today, by the balance among tectonics, weathering, and hydrothermal input. This early insight is remarkable. [Godd ris et al. \(2007\)](#) developed a climate-geochemical model and showed that the breakup of Rodinia caused a global climatic cooling of ca. 8°C. The increased length of the continental margins caused increased inorganic silicate weathering. The inorganic silicate weathering depends of course also on the geographical position of the continents. If the main part of the continents gathers at the poles or at one pole, then the climate is cooled, the precipitation is decreased and the silicate weathering is strongly diminished. However, the latter is the main component of pCO₂ sink ([Godd ris et al., 2007](#)). As a result, the CO₂ accumulates in the atmosphere and therefore the temperature rises. Thus, a negative feedback is created. If, on the other hand, the continents gather near the equator, silicate weathering is strongly stimulated and the CO₂ in the atmosphere decreases. The Neoproterozoic glaciations, Sturtian and Marinoan, comprehensively described by [Hoffman et al. \(1998\)](#), [Hoffman et al. \(2017\)](#), [Hoffman et al. \(2021\)](#), are also explained by [Donnadieu et al. \(2004\)](#) and [Godd ris et al. \(2007\)](#) in terms of the geographic location of Rodinia near the equator and the mechanism just outlined. (We will, however, propose a different mechanism for the Paleoproterozoic and Cryogenian glaciations in Subchapter 2.3. This, however, does not diminish the value of the theories presented here for the other parts of Earth's history). Thus, three items are inseparable in this main mechanism: (a) size and geographic position of the continents and height of the mountains, (b) long-term inorganic carbonate–silicate cycle, and (c) natural climate change. [Ramstein et al. \(2019\)](#) also emphasize the close link between tectonics, long-term inorganic carbonate–silicate cycle, and natural climate change. One must realize that the driving energy is the primordial heat of the Earth and the radioactive decay of ²³⁸U, ²³⁵U, ²³²Th, and ⁴⁰K in the mantle (see, e.g., [Walzer and Hendel, 2022](#)). This is because the amalgamation of continents into supercontinents, its subsequent breakup, and the formation of mountains is caused by thermal convection in the mantle. It is not a contrary mechanism to emphasize that plate motions including supercontinent amalgamation are driven by the negative buoyancy of mature oceanic lithosphere and feedbacks involving mantle convection driven by cooling where slabs are subducting and warming where plumes are rising ([Hoffman, 2014](#)). For [Walzer et al. \(2004\)](#), [Walzer et al. \(2006\)](#) show, the formation of the oceanic lithospheric plates and the subduction slabs are included in the mechanism and code described by [Walzer and Hendel \(2022\)](#).

We conclude this Section with an additional remark: Increased silicate weathering with increased length of post-rift continental margins occurs only to the extent that terrigenous sediment weathering is important. Other factors associated with supercontinent breakup are LIP (large terrestrial mafic igneous provinces) emplacement and greater rates of organic burial due to faster sediment accumulation rates. Higher fractional organic burial during Rodinia breakup is consistent with strongly ¹³C-enriched marine carbonate production for 100 Ma before the Sturtian snowball ([Halverson et al., 2018](#)).

2.2.2. Enhanced inorganic carbonate–silicate weathering caused by growth of the total mass of continents

In Section 2.2.1., we showed that the carbonate–silicate cycle can account for the faint young Sun paradox. However, it is unclear if this cycle can explain *all* aspects of natural climate variations over shorter periods, such as onsets and terminations, duration, and peculiar distribution of glaciations. Many studies have concluded that mountain building is directly associated with increased silicate weathering. For example, [Joshi et al. \(2019\)](#) reported that the late Paleozoic and present Cenozoic ice ages are linked to the Hercynian and Himalayan orogenies, respectively. The maxima of the glaciations lag behind the maxima of the timing of formation of low-latitude mountain chains by 10–20 Ma. Using the Intermediate Global Circulation Model 4, [Joshi et al. \(2019\)](#)

showed that the maxima of erosion, weathering, and temperature decrease follow each other. [Godd ris et al. \(2017\)](#) proposed that the biotic hypothesis for the late Paleozoic ice age needs to be reevaluated. Mountain building, continental drift, and silicate weathering were more important as cause for the drawdown of atmospheric carbon dioxide and the temperature decrease. [Godd ris et al. \(2017\)](#) used different variants of GEOCLIM models ([Donnadieu et al., 2006](#); [Godd ris et al., 2014](#)) and demonstrated that the contribution of the inorganic carbonate–silicate cycle to the consumption of CO₂ was greater than previously thought. Other authors had suggested that the onset of Late Paleozoic glaciation at 340 Ma was due to the expansion of land plants, which would have produced a decrease in atmospheric carbon dioxide. However, [Godd ris et al. \(2017\)](#) state that plant and carbon expansion substantially pre-dates glaciation. This argument is more important, in our opinion, because it is independent of the specific numerical model. [Godd ris et al. \(2017\)](#) conclude from their simulations that uplift of the Hercynian mountains and, as a result, inorganic carbonate–silicate weathering were crucial for the decrease of the CO₂ concentration in the air. In addition, if an ice age is not global, there is an additional effect ([Wan et al., 2017](#)). At low latitudes, such as the South China Sea, [Wan et al. \(2017\)](#) showed that sediments deposited during glacials were more weathered than those deposited during interglacials in the present ice age. [Wan et al. \(2017\)](#) explained this observation by intensified weathering of tropical shelf sediments during the lowstand conditions caused by large continental ice sheets. This additional effect is thought to be responsible for a ca. 9% reduction of CO₂ in the atmosphere.

The results just presented lead us to a new interpretation of Fig. 1 of [Walzer and Hendel \(2022\)](#). Since the upper red curve of this picture represents the computed juvenile contributions to the continent, we interpret the global detrital zircon age curves (lower panel) of [Puetz and Condie \(2019\)](#) to represent the actual juvenile contributions to the continents. This assumption is supposed because of the resemblance of the two panels of Figs. 1 and 7 of [Walzer and Hendel \(2022\)](#). We exclude ages older than 2900 Ma because the preservation is potentially incomplete or the crustal differentiation mechanisms were possibly different to those after 2900 Ma. The second possibility could be based on [van Kranendonk \(2010\)](#). He proposed that at 3500 Ma and earlier *two* types of crust had formed: high-grade gneiss terranes that contain evidence of a horizontal tectonic regime, and low-grade granite–greenstone terranes with predominantly vertical tectonic structures. The formation of granite–greenstone terranes during the Archean can possibly be explained by microphysical processes. The high temperatures during the Archean would have produced another style of subduction because of grain damage. Therefore, subduction was drip-like in many places ([Foley, 2018](#)). Similarly, [Gerya \(2019\)](#) proposed that prior to ca. 3 Ga, mantle temperatures were 200–250°C higher than today, resulting in a relatively ductile lithosphere and sporadically distributed episodic delamination. If the carbonate–silicate cycle was the main driver of ice ages, then an ice age should occur after each prominent peak in the global detrital zircon age distribution (Fig. 1). A large increase in silicate weathering would be expected after the high peak of the blue curve at 2700 Ma (Fig. 1). If a large amount of juvenile continental material was exposed to mechanical and subsequent chemical weathering, then one would expect a major ice age 10–30 Ma after the crustal growth peak. However, Fig. 1 does not reveal any ice age in the expected time interval. The moderate age peak of the dark green curve at about 2500 Ma, on the other hand, is followed by four ice ages. If [Hoffman \(2013\)](#) is correct, we only observe the Ramsay Lake, Bruce, and Gowganda ice ages. But this has no bearing on our conclusions. Between 2240 and 717.5 Ma there was no glacial epoch, but there are several maxima in the zircon age distribution. (The Kaigas diamictite is likely non-glacial. Evidence for glacial action comes from locations where the Numees (Sturtian) diamictite was incorrectly correlated with Kaigas ([Macdonald et al., 2010](#).) For about 600 Ma, we observe a marked peak of the yellow curve, for 600 Ma a peak of the red curve. However, the Sturtian and Marinoan ice ages occurred *before* these peaks. In the Phanerozoic, the correlations

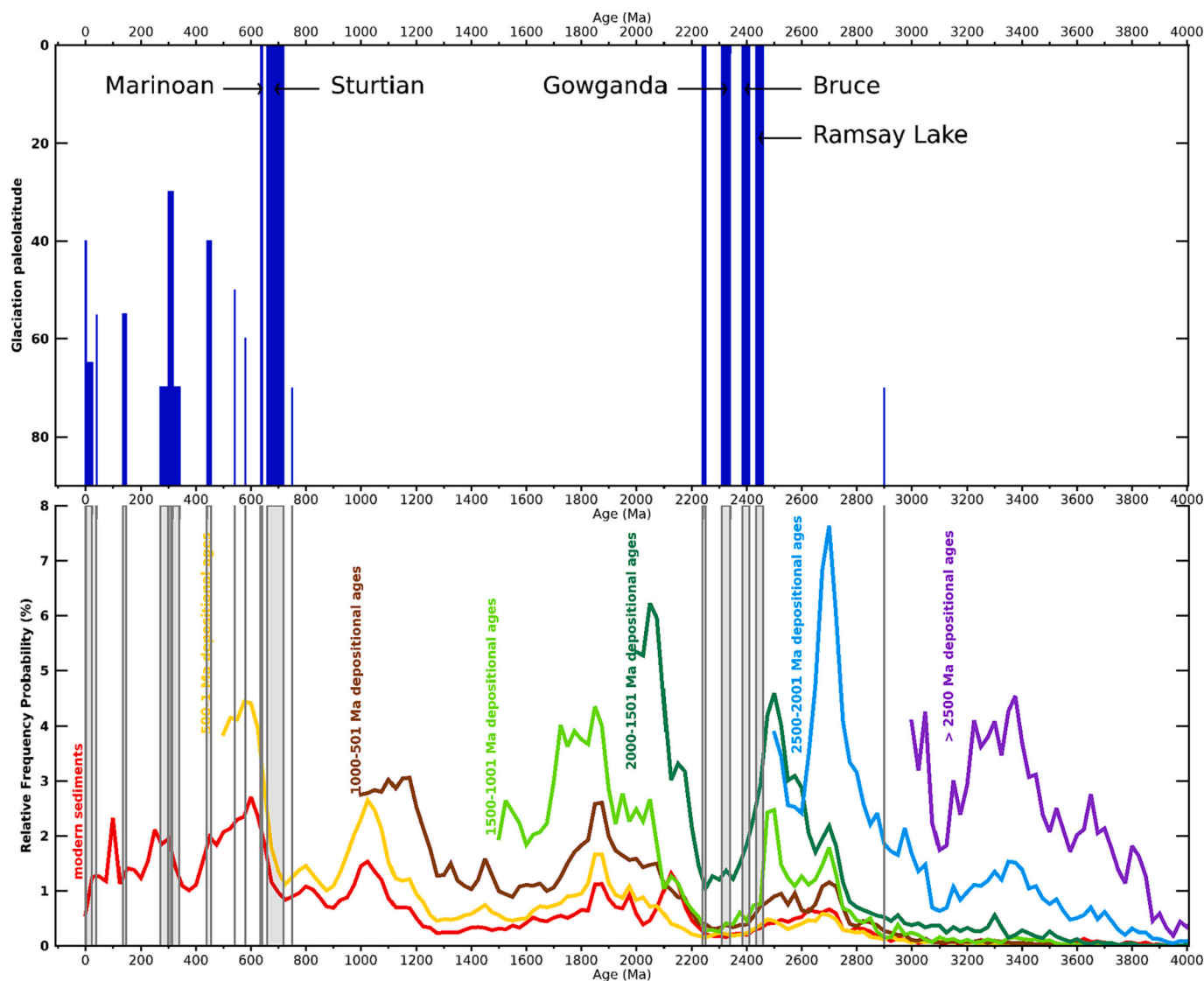


Fig. 1. The upper panel shows glaciations based on the data compiled in Section 3. The lower panel shows the observed global detrital zircon age curves of [Puetz and Condie \(2019\)](#). The grey vertical beams of the lower panel are useful for comparison. The colored curves are as follows: red = modern sediments; yellow = 500–1 Ma depositional ages; brown = 1000–501 Ma depositional ages; light green 1500–1001 Ma depositional ages; dark green = 2000–1501 Ma depositional ages; blue = 2500–2001 Ma depositional ages; purple = ages older than 2500 Ma. The Ramsay Lake glaciation corresponds to the Makganyene glaciation (compare [Fig. 14](#)). It is the only one of the Paleoproterozoic glaciations of which we can assume with some probability that it is a snowball Earth. The representation of the other three Paleoproterozoic glaciations is only a hypothesis, which is rather uncertain. Our main conclusions, however, are independent of whether this hypothesis is correct.

between the ice ages and zircon age peaks are also not clear. In our opinion, the findings do not show that the discussed mechanism does not work, but that other influences must also contribute, (compare Section 2.3.) so that the whole thing results from the superposition of different mechanisms.

2.2.3. Enhanced inorganic carbonate–silicate weathering caused by supercontinental breakup

The first supercontinent (Pangea) was identified by [Wegener \(1912\)](#), [Wegener \(1920\)](#). [Santosh et al. \(2009\)](#) proposed that the tectosphere as the buoyant keel of the continental crust is important in understanding continental fragmentation, dispersion, and amalgamation. This idea is also part of our model ([Walzer and Hendel, 2022](#)). [Yoshida and Santosh \(2011\)](#) proposed a mechanism to explain the episodic assembly and dispersal of supercontinents. [Nance et al. \(2014\)](#) reviewed the development of the concept of the supercontinent cycle in relation to the episodic nature of tectonic processes. Their history of the amalgamation and subsequent breakup of Rodinia is helpful for the following

discussion. [Hoffman et al. \(2017\)](#) showed that the Sturtian and Marinoan glaciations were coeval with the breakup of the supercontinent Rodinia. This resulted in an increase in the total length of continental margins. As such, the silicate weathering and carbonate sedimentation increased and the atmosphere became depleted in CO_2 . To evaluate these ideas, we used the temporal distribution of supercontinents from [Young \(2019\)](#) and compared it with our compilation of ice ages. [Fig. 2](#) shows marked ice ages during the breakup of the megacraton Laurascandia (four glaciations) and supercontinent Rodinia (two glaciations). There are four distinct Paleoproterozoic glaciations: three in the Huronian and the high-paleolatitude Rietfontein glaciation in South Africa, which postdates the youngest Huronian glaciation. *The breakup of Columbia (or Nuna) was NOT associated with an ice age.* This remarkable fact has already prompted many attempts at explanation. [Jellinek et al. \(2020\)](#), for example, believe to have found the explanation by means of a model in which a tectonically modulated carbon cycle model is coupled to a one-dimensional energy balance climate model. They propose that the relatively warm and unchanging climate of the Nuna

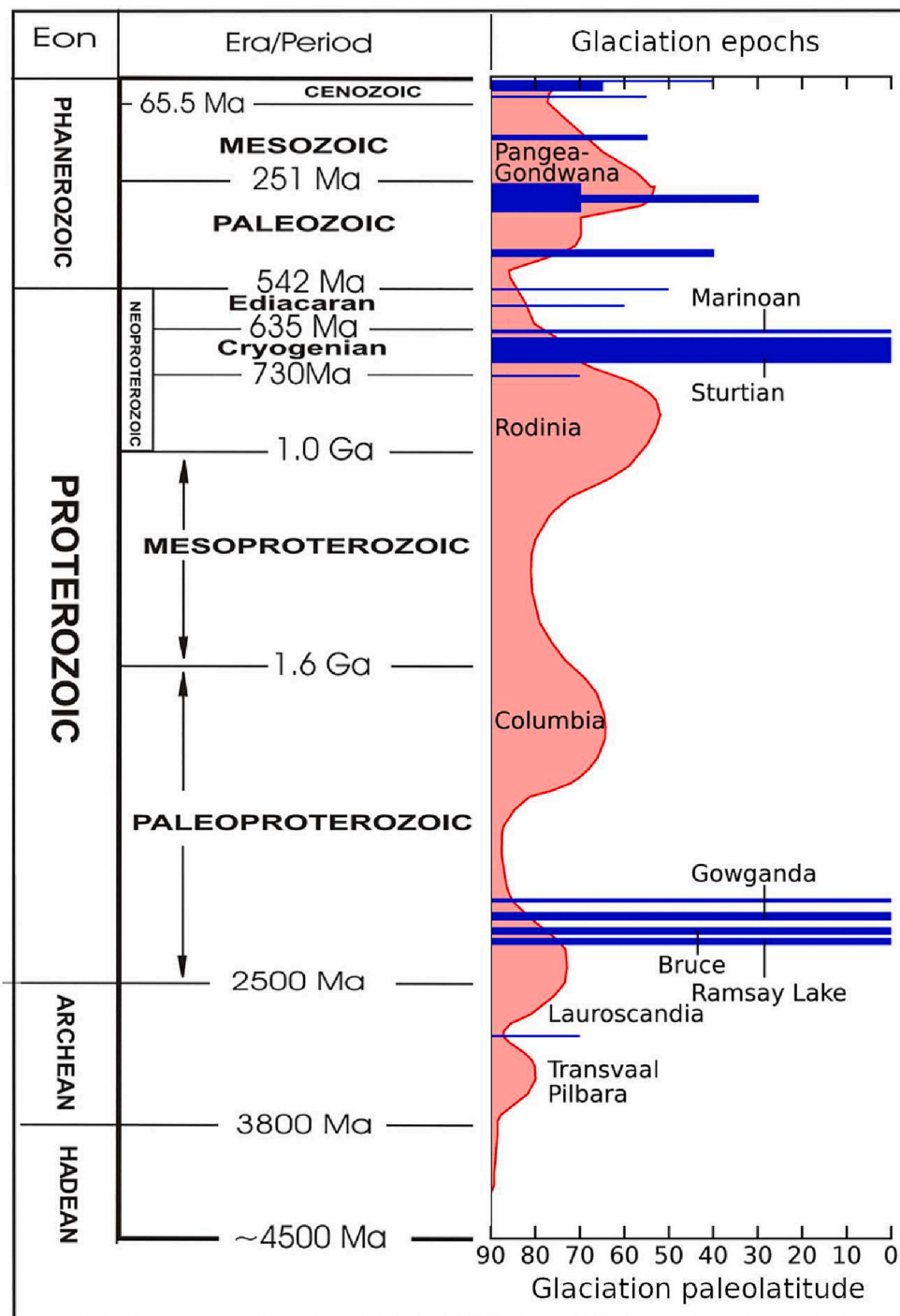


Fig. 2. Comparison of the distribution of supercontinents through time (Bleeker, 2004; Young, 2019) with ice ages based on the data compiled in Section 3. The Ramsay Lake glaciation corresponds to the Makganyene glaciation (compare Fig. 14). It is the only one of the Paleoproterozoic glaciations of which we can assume with some probability that it is a snowball Earth. The representation of the other three Paleoproterozoic glaciations is only a hypothesis, which is rather uncertain. Our main conclusions, however, are independent of whether this hypothesis is correct.

supercontinental epoch (1.8–1.3 Ga) is characteristic of thorough mantle thermal mixing. The model is quite complex, so we cannot evaluate it.

The Permian–Carboniferous glaciation occurred during the amalgamation of Pangea. The Cenozoic ice age is occurring *before* future supercontinent formation and breakup. The small glaciation after the Transvaal–Pilbara supercontinent breakup is not particularly convincing. Therefore, continental breakup enhanced inorganic silicate weathering is very likely not the most important mechanism to explain glaciations, but there must be other essential contributions. These inferences do not change if we compare the distribution of glaciations with a histogram of 100 000 detrital zircon ages from Voice et al. (2011) and

Cawood et al. (2013). If the breakup of Rodinia would generate two events at once, it would be incomprehensible why comparable large ice ages were not caused by the breakup of Pangea. Enhanced silicate weathering makes a significant contribution to atmospheric cooling, but this is obviously not sufficient to generate an ice age (Figs. 1 and 2).

An important criticism that affects both Sections 2.2.2. and 2.2.3. is the statement that zircons are products primarily of intermediate and felsic intrusive igneous rocks, whereas weathering rates are more sensitive to mafic and ultramafic extrusive igneous rocks. Macdonald et al. (2019) hypothesized that low-latitude arc-continent collisions drive cooling by exhuming and eroding mafic and ultramafic rocks in the warm, wet tropics, thereby increasing Earth’s potential to sequester

carbon through chemical weathering.

2.3. Volcanic hypotheses

It is obvious that onsets and terminations of major glaciations are abrupt (Hoffman et al., 2017; Hoffman et al., 2021). Therefore, attempts to explain these phenomena by inorganic carbonate–silicate weathering are hopeless. Consequently, we compared the temporal distribution of all known LIPs based on Ernst (2014) and Ernst and Youbi (2017) (Fig. 3) with the sequence of glaciations. At first glance, this comparison does not support a close relationship between LIPs and glaciations. In the long period between the last Paleoproterozoic glaciation and the first Cryogenic snowball Earth period, there were numerous LIPs but no ice ages. Even if we consider only the late Proterozoic and recent geologic history since the beginning of the Sturtian snowball period, there is no systematic correlation between LIPs and onsets and terminations of glaciations. Macdonald et al. (2010) suggested that the age of the glacial deposits of the Upper Mount Harper Group (716.47 ± 0.24 Ma) is indistinguishable from the age of the Franklin LIP (716.33 ± 0.45 Ma). They concluded that the Franklin LIP basalts caused strong drawdown of atmospheric CO₂ and triggered the Sturtian snowball Earth epoch. Macdonald and Wordworth (2017) suggested that the Sturtian snowball Earth epoch was initiated by SO₂ and H₂S outgassing into the stratosphere, and that concurrent CO₂ emissions are relatively small. SO₂ and H₂S produce sulfates. Formation of stratospheric aerosols causes an increase in albedo, which reduces incoming solar irradiation. As Macdonald and Wordworth (2017) emphasized, Franklin LIP is a special case because, first, it is enormous and was erupted squarely across the paleoequator, where stratospheric aerosol injection has the strongest

cooling effect, and second, because Franklin LIP lavas are exceptionally sulfur-rich because they were erupted through sulfate-evaporite bearing Neoproterozoic strata (Shaler Group). For aerosol to reach the stratosphere at the equator requires long-lived thermal plumes above lava fountains, as are observed in Iceland. This is an indication that it is not sufficient to simply look at the distribution of LIPs over the time axis. One must consider the connection with physical climatology (Imbrie and Imbrie, 1986). The closer the LIPs are to the paleoequator, the greater the impact on climate. Furthermore, Gumsley et al. (2017) proposed that LIPs play an important role in the rise of oxygen and in both initiating and terminating glaciations. They suggested that the Great Oxidation Event (Anbar et al., 2007; Sverjensky and Lee, 2010; Catling, 2014; Schirrmeister et al., 2015; Warke et al., 2020) could be subdivided into several sub-events, and postulated that atmospheric oxygen oscillations had occurred, which might explain the chronology of the Paleoproterozoic glaciations. McKenzie et al. (2016) proposed that CO₂ emissions from continental arcs have controlled the climate since ca. 720 Ma, although the effects of SO₂ and H₂S were not discussed. At first glance, the hypotheses of McKenzie et al. (2016) and Macdonald and Wordworth (2017) seem to contradict each other. However, a closer look reveals that they are not necessarily in conflict because arc magmatism is generally far more CO₂ rich than flood-basalt magmatism, although the latter is variable depending on plume-head eclogite content and the nature of crustal wallrocks. The Macdonald and Wordworth (2017) hypothesis states explicitly that a preexisting cold climate is a precondition, in order to lower the height of the tropical tropopause. This could rule out the effects of many if not most LIPs between ca. 800 and 2230 Ma. The currently favoured connection between Sturtian glaciation and Franklin LIP volcanism is through LIP

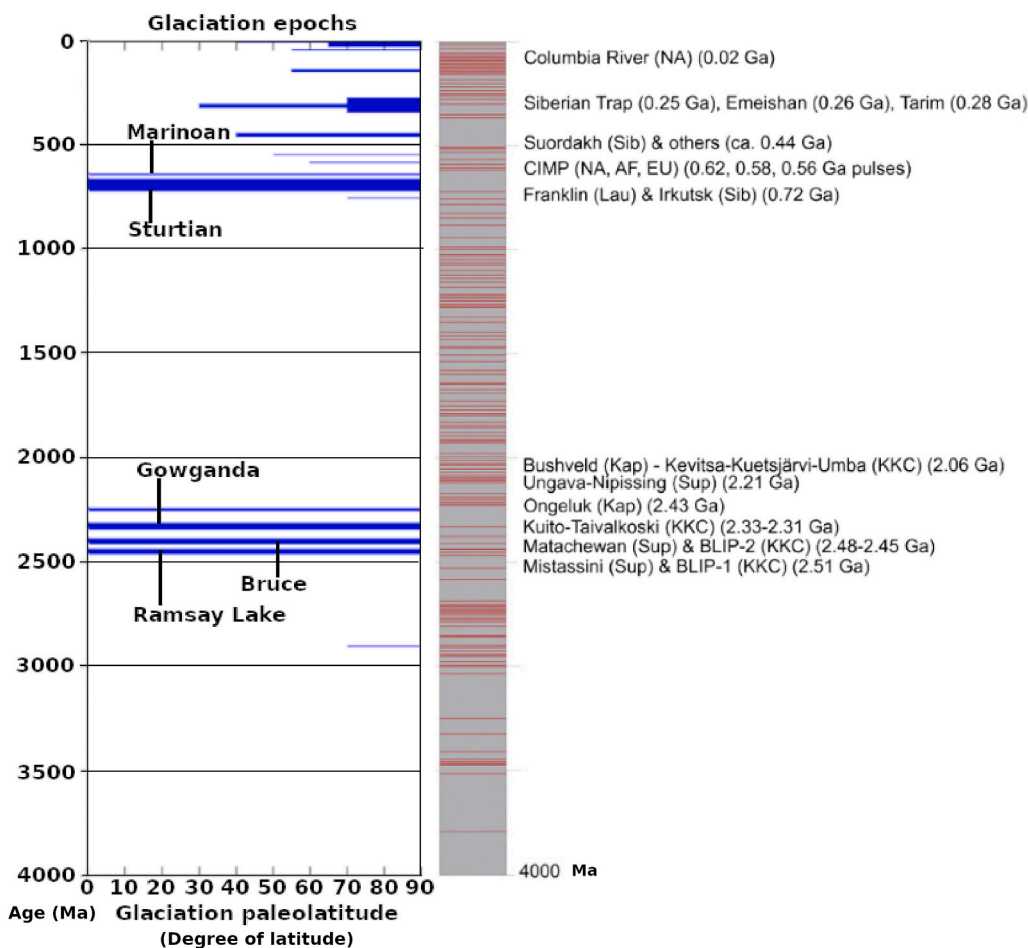


Fig. 3. Comparison of the timing of glaciations with the LIP record of Ernst and Youbi (2017). The Ramsay Lake glaciation corresponds to the Makganyene glaciation (compare Fig. 14). It is the only one of the Paleoproterozoic glaciations of which we can assume with some probability that it is a snowball Earth. The representation of the other three Paleoproterozoic glaciations is only a hypothesis, which is rather uncertain. Our main conclusions, however, are independent of whether this hypothesis is correct.

weathering (Cox et al., 2016). Franklin LIP weathering would be greatly intensified by its location in the hot-humid equatorial zone (15°N–15°S). The weathering hypothesis is now favoured because improved geochronology constrains Franklin LIP volcanism to ≤ 1.0 Ma duration centred on 719 Ma, whereas the onset of Sturtian snowball Earth period is at 717 Ma (Pu et al., 2022). Youbi et al. (2020) show that magmatic provinces can have a significant impact on global climate. They conclude that the age of pulses from the Central Iapetus magmatic province (580–570 Ma) is consistent with the Gaskiers glaciation, and hypothesize that, first, the initial siliciclastic pulse (ca. 580 Ma) of the Ouarzazate event (Anti-Atlas of Morocco) helped trigger the Gaskiers glaciation, and second, global warming associated with subsequent ca. 579–570 Ma continental flood basalts marking the second phase of the Ouarzazate event helped trigger the Gaskiers glaciation. 579–570 Ma continental flood basalts, marking the second phase of the Ouarzazate event, contributed to the end of glaciation. Next, Youbi et al. (2021) investigate this promising mechanism for larger temporal and spatial domains. They investigate the correlation of LIPs with major glaciation events, focusing on those from the Neoproterozoic and Phanerozoic. We conclude this Section by noting that of the proposed mechanisms to explain the abrupt onsets and terminations of major glaciations, particularly snowball Earth periods, the LIPs are the most likely to be in question. Fig. 3 shows, however, that this conclusion cannot be valid without additional conditions. The effects of the eruptions of the LIPs have to be seen in connection with the physical climatology at the time of the eruption, the proximity of the LIPs to the paleoequator, the strength of the eruption and the chemical composition of the lava and the emitted gases.

2.4. Biotic theories and the Great Oxidation Event

Numerous studies have proposed that natural climate change and glaciations are caused by biotic factors. Kopp et al. (2005) argued that oxygen-producing cyanobacteria evolved rapidly, destroyed the methane greenhouse state, and triggered a snowball Earth period within about 1 Ma. With increasing oxygenation, methane reacted with oxygen, and H₂O and CO₂ were produced. H₂O and CO₂ are less powerful greenhouse gases than methane. Because the proposed mechanism requires oxygen, Kopp et al. (2005) assumed that the process occurred shortly before the Makganyene snowball Earth epoch. However, the consensus view among biogeochemists and molecular phylogenomicists is that cyanobacteria evolved hundreds of Ma before the Great Oxidation Event (GOE), and that oxygenic photosynthesis may be more primitive than anoxygenic photosynthesis (Cardona et al., 2019; Cardona, 2019). Knoll (2014) described the slow expansion of eukaryotic organisms in the oxygenated surface waters of Proterozoic oceans, which led to a major eukaryotic diversification at about 800 Ma. Based on similar observations, Feulner et al. (2015) proposed that the final rapid expansion of eukaryotic algae caused the formation of organic cloud condensation nuclei, which contributed to the Sturtian and Marinoan snowball Earth epochs. Presently, eukaryotic algae are the main source of cloud condensation nuclei over the oceans because they generate dimethylsulfoniopropionate (DMSP). Therefore, the present-day marine sulfur flux exceeds the sulfur flux of volcanic origin. At approximately 675 Ma, proto-haptophytes had probably developed the capability to generate DMSP. Feulner et al. (2015) proposed that this resulted in the relatively rapid augmentation of biogenic sulfur aerosols, acidified rainwater, and decrease in atmospheric CO₂ concentrations at the beginning of the Cryogenian. However, it should be noted that 675 Ma is 42 Ma after Sturtian snowball onset. Major groups of archaeplastid algae were already distinguished and multicellular by 1.0 Ga. The diversification of eukaryotes after ~800 Ma (Knoll et al., 2006) is mainly of protistan heterotrophs, i.e. vase-shaped microfossils interpreted as testate amoebae, which most probably do not produce DMSP. This is why the Feulner et al. (2015) hypothesis was referred to as good idea lacking empirical evidence. Macdonald and Wordsworth (2017)

critiqued Feulner et al. (2015) as follows: “Albedo changes due to the emergence of eukaryotic algae rely on the coincidence of a putative evolutionary milestone for which there is no evidence.” They noted that the Franklin LIP coincided with the onset of the Sturtian snowball Earth epoch. The Franklin LIP was special in a number of different respects. Feulner (2017) used the climate model of Montoya et al. (2005) to explain climate change near the Carboniferous–Permian boundary. This model combines an ocean circulation model, a fast atmosphere model, and a dynamic sea–ice model. The high burial rate of organic carbon related to the formation of anthracite coal caused significant drawdown of atmospheric CO₂ during the Carboniferous (358.9–298.9 Ma). In addition, Feulner (2017) modeled the effects of the slight variations of the present-day obliquity, eccentricity of Earth’s orbit, and lunisolar precession on the evolution of atmospheric CO₂ for the interval from 308.4 to 301 Ma. Feulner (2017) concluded that cooling brought Earth close to the limit of a snowball Earth at ca. 300 Ma. This conception had some forerunners e. g. Berner (2004). However, Godd eris et al. (2017) proposed that biotic factors do not cause the Permian–Carboniferous ice age, and highlighted the colonization of the continents by vascular plants in the Late Devonian, which was long before the Permian–Carboniferous ice age. Godd eris et al. (2017) proposed that enhanced carbonate–silicate weathering induced by uplift during the Hercynian orogeny and assembly of Pangea caused the late Paleozoic ice age. Compare our Section 2.2. Based on the evidence, we suggest that biotic evolution influenced climate and glaciations only to a small extend. One of the earliest and most popular explanations, but one lacking strong empirical support, is a microbially mediated increase in terrestrial weathering rates. The empirical basis was said to be a late Tonian increase in clay mineral production (Kennedy et al., 2006), but the clays later turned out to be detrital mica and their increase coincided with the Sturtian glaciation (Tosca et al., 2010).

Holland (2002) used the term Great Oxidation Event (GOE) for the transition of atmosphere from a reducing to an oxidizing state. Prior to the GOE, all sulfur gases were reduced to pyrite. Kump (2008) described how the atmosphere obtained a considerable percentage of oxygen. Because rocks older than ca. 2450 Ma exhibit a large degree of mass-independent fractionation (MIF) of sulfur isotopes and the mean variation of $\Delta^{33}\text{S}$ values rapidly virtually vanishes for younger rocks, the GOE was thought to be a relatively sudden event. Fig. 4 shows the abrupt end of the period of large variations in $\Delta^{33}\text{S}$ values. The large variations before the GOE were probably produced by photochemical reactions of SO₂ and H₂S ejected from volcanoes into the atmosphere. This process cannot continue if O₂ concentrations exceed a certain threshold, which is perhaps less than 0.001% of the present-day atmospheric level (Pavlov and Kasting, 2002). Lyons et al. (2014) proposed that the growth of the atmospheric abundance of O₂ proceeded and that oxygenic photosynthesis was the only important source of free oxygen at the surface of the Earth. They suggested that atmospheric reorganization was driven mainly by biological productivity, and that cyanobacteria were particularly important because these organisms were the earliest producers of free O₂ by photosynthesis. The black curve of the lower panel of Fig. 4, representing the $\delta^{13}\text{C}$ evolution, indeed shows that the traditional GOE occurred long before the strong $\delta^{13}\text{C}$ fluctuations in the early Proterozoic. The great time lag between these fluctuations in the early Proterozoic and the strong $\delta^{13}\text{C}$ fluctuations in the late Proterozoic has been explained by the hypothesis that, in the beginning, only the topmost layer of the ocean incorporated O₂ in solution whereas the deep ocean was free of oxygen and enriched in H₂S (Canfield, 1998) and that this anoxic part of the ocean degraded the abundances of bioessential elements and thus promoted the diversification of eukaryotic organisms leading to a final big increase of oxygenation followed by a strong expansion of life (Lyons et al., 2014). We compared our compilation of ice ages (upper panel of Fig. 4) with the $\delta^{13}\text{C}$ curve from Lyons et al. (2014), and identified that the first large positive excursions clearly occurred after the Ramsey Lake, Bruce, and Gowganda snowball Earth

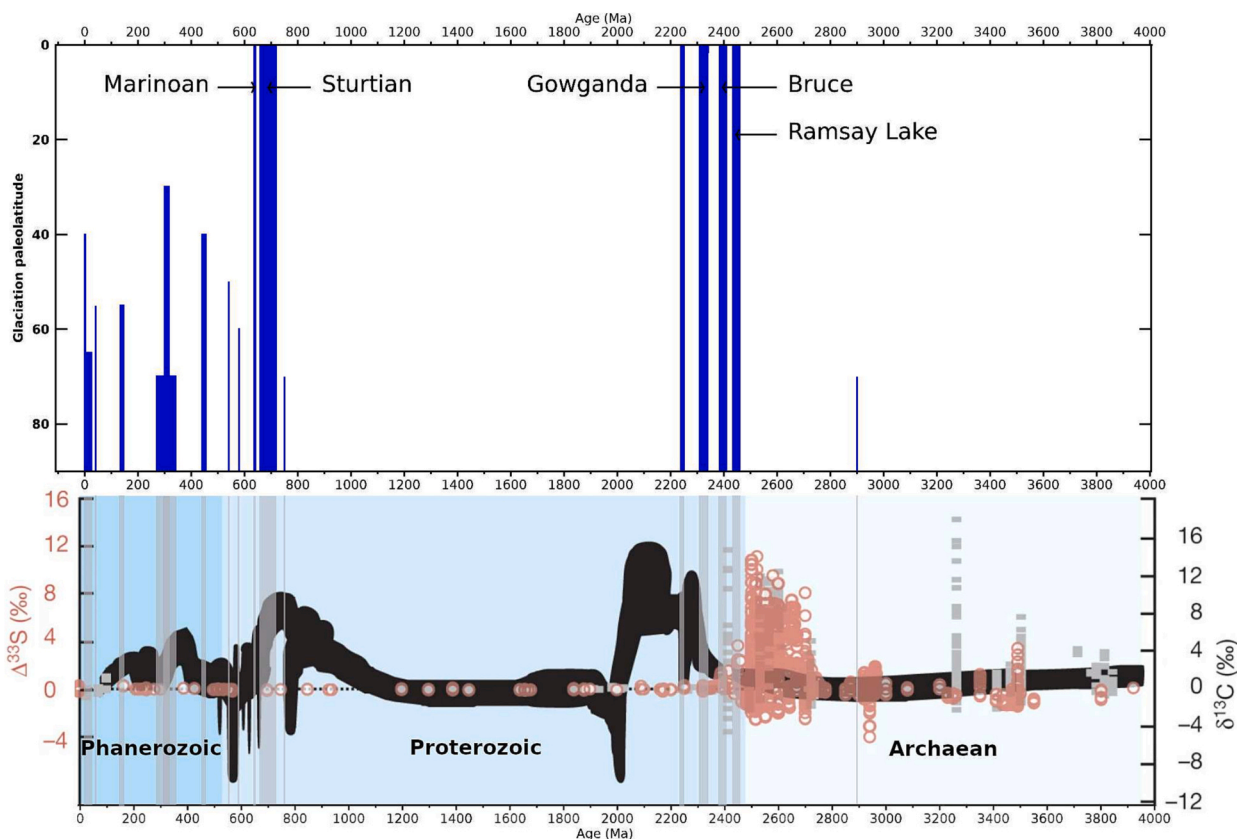


Fig. 4. The upper panel shows ice ages in the past 4 Ga, where the vertical height of each blue bar signifies the minimum paleolatitude of ice extent. The data are provided in Section 3. The lower panel shows $\delta^{13}\text{C}$ (black) and $\Delta^{33}\text{S}$ ($=\delta^{33}\text{S} - 0.515 \cdot \delta^{34}\text{S}$) values for the past 4 Ga. The isotope data are from Lyons et al. (2014), Reinhard et al. (2013), and Planavsky et al. (2012). The $\Delta^{33}\text{S}$ values from secondary ion mass spectroscopy (SIMS) are shown in gray, whereas the other sulfur isotope data are indicated by red circles. The Ramsay Lake glaciation corresponds to the Makganyene glaciation (compare Fig. 14). It is the only one of the Paleoproterozoic glaciations of which we can assume with some probability that it is a snowball Earth. The representation of the other three Paleoproterozoic glaciations is only a hypothesis, which is rather uncertain. Our main conclusions, however, are independent of whether this hypothesis is correct.

epochs, whereas the temporal order is *reversed* in the case of the second largest maximum of the $\delta^{13}\text{C}$ curve in the late Proterozoic, with respect to the Sturtian and Marinoan snowball Earth epochs. The fourfold subdivision of the Paleoproterozoic ice ages and the twofold subdivision of the Cryogenian ice ages are not reflected in the $\delta^{13}\text{C}$ curve.

The uniform $\delta^{13}\text{C}$ values between 1.9 and 1.0 Ga (Fig. 4) are difficult to explain. Daines et al. (2017) attempted to model this period by taking into account erosion, weathering, and biogeochemical cycling. Their results exhibit a strong negative feedback when the atmospheric O_2 concentration was $\text{pO}_2 \sim 0.1$ PAL (present atmospheric level). The stability no longer exists at $\text{pO}_2 < 0.01$ PAL. Between these boundaries, the $\delta^{13}\text{C}$ record is insensitive to variations in the burial rate of organic carbon. Daines et al. (2017) concluded that elevated biological productivity and subsequent carbon burial caused the GOE. Our representation in Fig. 4 is supported by Warke et al. (2020), who show that the GOE in northwestern Russia occurred between 2501 and 2434 Ma, while the Ramsay Lake ice age occurred between 2460 and 2435 Ma. This means that neither the first Paleoproterozoic glaciation nor the later Paleoproterozoic glaciations can be the cause of the GOE. The strong push in the evolution of oxygenic photosynthesis, the GOE, as monitored by the S-MIF/S-MDF transition preceded the four Paleoproterozoic snowball Earth intervals. At least, this would be the case if the $\Delta^{33}\text{S}$ values of Planavsky et al. (2012), Reinhard et al. (2013), and Lyons et al. (2014) are correct.

In addition to the observations and hypotheses presented in Section 2.4. above, the following critical remarks must be made: The Canfield (1998) deepwater euxinia hypothesis was conceived to explain the

absence of banded iron-formation after 1.85 Ga, except for Cryogenian snowballs, despite evidence for persistent deepwater anoxia. It is difficult to see the connection between deepwater euxinia and absence of C-isotope excursions. Near zero permil $\delta^{13}\text{C}$ during the 'boring billion' implies fractional organic burial similar to modern. Subsequent to Canfield (1998), many studies have shown that Proterozoic deepwaters were prevalently ferruginous, and euxinic only locally around large deltas sources of riverine sulfate input. Accordingly, lack of bioessential, i.e. nutrients due to widespread euxinia (Anbar and Knoll, 2002) does not apply. The fundamental problem is to explain why atmospheric O_2 levels did not approach modern and remain there soon after the GOE, as Holland (2002) originally expected. That problem remains unresolved. Furthermore, it should be noted that correlations between C-isotope excursions (CIEs) and Paleoproterozoic glaciations are highly speculative. There are few C-isotope records from the period of Huronian and Transvaal glaciations. During the Neoproterozoic, large CIEs occurred before, between and after the Cryogenian snowballs. This cannot be described as "the reverse" of the Paleoproterozoic. A more obvious distinction is that only positive CIEs are observed in the Paleoproterozoic, where both positive and negative CIEs characterize the Neoproterozoic after ~ 870 Ma. Not that we expect CIEs to become progressively dampened at older ages because of increased dissolved inorganic carbon (DIC) reservoir size with higher atmospheric pCO_2 . Any given change in the organic export flux from the surface ocean would have a smaller isotopic effect if the DIC reservoir is larger.

2.5. Proterozoic ice ages on a high-obliquity Earth

In Sections 2.2 through 2.3 we have presented hypotheses that are very likely to explain significant portions of natural climate change. At this point, however, we discuss a fourth proposal that, to be clear, we do not believe to be valid.

Williams (1975) and Williams et al. (2016) presented empirical evidence that supports the hypothesis of Proterozoic ice ages at low paleolatitudes. This includes periglacial deposits, thermal contraction cracks caused by severe frost, and annual oscillations in sea level recorded by tidal rhythmites. Therefore, at least after Williams et al. (2016), open ocean must have been present at this time, along with strong seasonality. Meter scale periglacial sand wedges were observed. Therefore, Williams et al. (2016) suggested that the *unmodified* snowball Earth hypothesis is incorrect. They continued with a bold statement and suggested that obliquity was greater than 54° during the Proterozoic ice ages. Similarly, Young (2018) suggested that prior to the Ediacaran, Earth's rotational and orbital axes were separated by a high angle (greater than 54°) and, therefore, Proterozoic ice ages were caused by the breakup of supercontinents, whereas after a catastrophic event, perhaps an impact, the obliquity obtained values oscillating between 22.1° and 24.5°. Young (2018) proposed that Proterozoic ice ages were caused in a completely different way than today by orogenic activity associated with *collisions* during amalgamation of a new supercontinent.

There are plenty of arguments against the high-obliquity hypothesis. The following can be said about the so-called 'annual oscillation in sea level'. In William's analysis, there is an annual signal in the Elatina tidal record, but these are records of oscillatory tidal currents, e.g., in tidal channels, more than of sea level. - The presence of tidal rhythmites does not require open water. Tides in the ocean are not impeded by a thin skin of ice. The ice shell itself is subject to the same gravitational forces and orbital centrifugal forces. In fact, it has been argued that the presence of a continuous ice cover accounts for the perfect preservation of William's tidal bundles, by eliminating interference from wave action. Strong seasonality (polygonal sand-wedges) at low paleolatitude was what drove the high-obliquity hypothesis. In its original form, obliquity was inferred to have chaotically varied between high and low values, with high obliquity favouring glaciation, because of stronger ice albedo feedback due to larger zonal area at lower latitude, and low-latitude ice. Findings from the celestial mechanics of the solar system caused Williams (1975) to revise his model to one of perpetual high obliquity until after Marinoan time, when it rapidly decreased to low values by Cambrian time, when paleoclimate is known to have been warmest at the equator. - No climate dynamicist would agree that high-obliquity is a credible hypothesis for low-latitude glaciation at sea level. High obliquity results in strong seasonality and hot summers everywhere. The coupled ocean-atmosphere-sea ice MIT-climate change model (GCM) was unable to simulate partial ice cover with large obliquity (Ferreira et al., 2014). They found only two climate states are stable as radiative forcing is varied: nonglacial and panglacial. -

It should be mentioned that high obliquity does not account for physically abrupt onsets and terminations of Cryogenian glaciations, their common association with thick shallow-marine carbonate successions indicating a geographically warmer part of the surface ocean, the presence of characteristic postglacial cap carbonates, or association with the only regional-scale sedimentary iron-formations in the past 1.85 Ga. Further empirical evidence against Proterozoic high-obliquity was marshalled by Evans (2006), showing that paleolatitudes of evaporite deposits remained statistically unchanged over the past 2.0 Ga, whereas high-obliquity would reverse the Hadley circulation resulting in an equatorial zone of largest net evaporation. -

What about strong seasonality at low paleolatitude, Williams original motivation? Snowball Earth itself greatly increases seasonality because the solid surface has little thermal inertia. This strong seasonality does not prevent glaciation, as argued above against high-obliquity, because it only occurs after the tropical ocean had already frozen over. Still,

Williams argued that snowball models did not produce large enough seasonality to explain his Cattle Grid Mine permafrost structures. It turned out that this was because most climate models, which evolved for global change research, incorporated the present near-circular orbit. When the full range of eccentricity was included, low-latitude seasonality at low obliquity and an ice-covered produced seasonality large enough to satisfy Williams' specifications (Liu et al., 2020). - Due to cold surface temperature resulting from high albedo, the polar ice caps thicken to the point where they flow equatorward like an ice shelf. At the low CO₂ of a snowball onset, the sea-glaciers are ca. 1.0 km thick, with ≤100 m thickness variation due to flow. As a result, the flow tends to seal off any area of open water or thin ice. This is very different than Kirschvink's (1992) conception of floating pack-ice. Key papers were written by Warren et al. (2002), Goodman and Pierrehumbert (2003), Li and Pierrehumbert (2011), Tziperman et al. (2012), and Goodman and Strom (2013). Models with stable waterbelt solutions without sea-ice dynamics commonly lapse to snowballs when ice dynamics are included (Voigt and Abbot 2012). Stable waterbelt solutions, i.e., stable low-latitude marine ice margins, have been sought in coupled models for obvious reasons. It is important to point out that the stable waterbelt branch in bifurcation diagrams of such models resides inside the snowball CO₂ hysteresis loop. As a result, the stable waterbelt state cannot be reached from any other state. If the waterbelt state inaccessible from other states, it has no relevance for geology (Braun et al., 2022). Pierrehumbert et al. (2011) summarized the opinion among climate dynamicists that for a waterbelt state to have been stable over the millions of years of Cryogenian snowballs, given periodic and stochastic changes, is implausible. There are other solutions for the survival of the eukaryotes (Vincent et al., 2000; Vincent et al., 2004; Hoffman, 2016; Hawes et al., 2018).

Apart from the geological objections to the hypothesis of Williams et al. (2016), it is difficult to explain the sudden change in obliquity. A major impact would probably have generated other catastrophic effects, which have not been observed. There are also some other geological objections. For example, Hoffman and Li (2009) showed that six of eight occurrences of Cryogenian periglacial sand wedges are located at paleolatitudes greater than 30°. Their discussion is based on a study of the formation and breakup of Rodinia by Li et al. (2008). Donnadieu et al. (2004) calculate a spreading polar cap of glacier ice with a thickness that can reach several kilometers, with a wet base. These modeled polar caps move from the poles to the equator in the Paleoproterozoic and in the Cryogenian, as they do today. Laskar et al. (1993) found a large chaotic zone between 60° and 90° obliquity. In the present-day, there is no such chaotic zone on Earth, and there are only small variations around the present-day value of 23.43663°. The Moon has stabilized Earth's obliquity. Colose et al. (2019) used the NASA GISS ROCKE-3d fully coupled atmosphere-ocean Global Climate Model to examine whether low- or high-obliquity planets are more likely to experience a planet-wide ice age. They demonstrated that *high-obliquity planets remain considerably warmer* than their low-obliquity counterparts, other things being equal. Although equatorial glacial belts are stable at high obliquity, it is more difficult to develop a global glaciation. Hoffman et al. (2017) showed that the present-day distribution of Sturtian and Marinoan glacial and periglacial deposits is rather uniform. When these observations are incorporated into paleogeographic reconstructions, the glacial observations are likewise *not* restricted to the equatorial climate zone. Based on the discussion above, the high-obliquity hypothesis has little merit. Proterozoic ice ages started as usual at the poles and propagated towards the equator.

3. Snowball Earth and glaciations

3.1. Snowball Earth

Here we distinguish the concepts of the snowball Earth and glaciation. Only in the Early Paleoproterozoic and Neoproterozoic records we

find snowball Earth periods when *all* oceans were ice-covered, allowing for meltwater drainage and air-gas exchange through cracks and moulines, and partial ice cover on land. All ice-sheet-atmosphere general circulation models (GCMs) with completely ice-covered oceans simulate ice-free land areas where there is net surface ablation. Le Hir showed, counterintuitively, that ice-free continental area increases as atmospheric CO₂ rises and the surface warms (Benn et al., 2015). Ice-free land surfaces during Cryogenian glaciations were recognized from polygonal sand wedges and permafrost involutions in many areas from the 1960s onward. Snowball Earth is a climate state driven primarily by ice-albedo. Consequently, it is fundamentally an oceanographic phenomenon. This is because, first, the oceans cover a much larger area than the continents, and second, the albedo contrast between seawater and multiyear sea-ice is greater than that between bare ground and glacial ice, and third, ice forms wherever the ocean surface cools below a critical temperature, whereas the low albedo of a frozen land surface may persist ice-free where there is net ablation. On snowball Earth, net accumulation at higher elevations and latitudes is balanced by net ablation elsewhere. A distinguishing secondary characteristic of the snowball climate is the equatorial zone of net ablation, in contrast to the subtropical deserts of all other climate states. The equatorial desert on snowball Earth is a consequence of the solid surface (Voigt, 2013). However, an ice age or glaciation is a long period of reduction in the temperature of the surface of the oceans and the continents and in the atmosphere during which there are polar ice sheets and high mountain glaciers. As such, every snowball Earth epoch was an ice age but not vice versa. Another distinction is important. Individual pulses of cold climate *within* an ice age are called glaciations, separated from each other by warmer periods, which we call interglaciations.

Harland (1964) suggested an extreme ice age prior to the Cambrian, which formed marine tillites in the tropics. The CO₂-driven escape from the snowball state was first laid out by a Walker et al. (1981) paper on temperature-dependent silicate weathering as a climate-stabilizing feedback. Kirschvink (1992) was the first to apply the self-reversing ice-albedo bifurcation concept to the geological record, and he introduced the name 'snowball Earth' as an allusion to its appearance from space. Actually, the presence of an ice sheet allows weathering beneath it to continue. An ice sheet forms a insulating blanket that allows geothermal heat to raise temperature to the melting at the base of the ice, even where surface air temperatures are −50°C as in central Antarctica. The ground beneath an ice sheet is highly reactive because of abundant freshly-ground rock powder produced by glacial abrasion. In contrast, virtually no weathering occurs in polar deserts where the land surface is directly exposed to cold air. Also, sea-floor weathering continues to consume CO₂ although at a slow rate due to very cold seawater temperature on snowball Earth. Nevertheless, the Walker et al. (1981) self-reversing snowball still holds because CO₂ consumption rate was less than the outgassing flux (Hir et al., 2009). A more basic reason for CO₂ accumulation in a snowball climate is that CO₂ gas is not soluble in snow, only in liquid precipitation. If there was no rain, there was no mechanism to scrub CO₂ from air short of direct condensation during polar winter, most of which sublimates away during polar summer. Hoffman et al. (1998) and Hoffman and Schrag (2002) made some key observations that were linked to the snowball Earth: Negative $\delta^{13}\text{C}$ excursions were detected in carbonate rocks located above and below glacial deposits in Namibia. The Neoproterozoic snowball onsets are synchronous, remarkably within a few hundred years, at low paleolatitudes and terminations are synchronous at all paleolatitudes. There could be a slow increase in ice cover before the snowball bifurcation threshold was reached. Terminations are predicted to be globally synchronous because of intrinsic CO₂ hysteresis (Walker et al., 1981). Existing geochronological data are virtually all from paleolatitudes $\leq 35^\circ$. Early models implied that a snowball albedo could not be overcome by geologically realistic CO₂ levels (Pierrehumbert, 2005), but this problem was resolved when the effects of clouds, in particular net warming in a snowball climate, are explicitly modelled (Abbot et al., 2012; Abbot

et al., 2013; Abbot, 2014). Each snowball Earth termination was connected with an intense greenhouse phase characterized by a flux of alkalinity leading to the deposition of a cap dolostone layer. In general, overlying this is a sequence of mixed sediments that are also carbonate-dominated. Such observations are global and particularly concentrated near the equator. We want to elaborate on that a bit more. During a snowball, an enormous dissolved inorganic carbon (DIC) reservoir builds up in the snowball ocean because detrital carbonate, delivered as rock powder in the runoff of the meltwater beneath ice sheets eroding tropical carbonate-rich continental shelves and platforms, is slowly dissolved to buffer rising seawater acidity from CO₂ outgassed at mid-ocean ridges. When the snowball deglaciates, the ocean warms, continental shelves are flooded, and pH value slowly rises again, the surplus DIC reprecipitates as carbonate, sufficient in volume to cover the entire continental area with an average of 3–5 m of carbonate rock (Hoffman and Schrag, 2002; Higgins and Schrag, 2003). However, the story is not so simple because snowball deglaciation results in a surface ocean dominated by glacial meltwater, not the alkalinity-charged snowball brine (Shields, 2005), although vertical mixing would be focussed at continental margins where many cap dolomites are preserved and exposed. Therefore, rapid syndeglacial weathering is required to drive the meltwater lid to critical oversaturation. Because of the short time-scale, the syndeglacial alkalinity flux from weathering must have been dominated by carbonate weathering (Higgins and Schrag, 2003), since carbonates dissolve much faster than silicates and because many carbonate shelves and platforms would initially have been subaerial exposed during deglaciation. It is not possible to cover all aspects of the snowball Earth hypothesis here, but a detailed review can be found in Hoffman et al. (2017), Hoffman et al. (2021).

3.2. Glaciations

An ice age or glaciation is divided into a series of glaciations and interglaciations. The latter ones can be explained by the Milankovitch hypothesis (Berger, 1988), although there are objections (e.g., Paillard, 2015). It should be noted that a part of the the Milankovitch (1941) hypothesis is that glacier growth is favoured by cool summers at 65°N in the Quaternary. For the time being, we will only outline the main features of Milankovitch hypothesis. There are three Milankovitch cycles that affect the climate: (1) eccentricity variations of Earth's orbit with a combined main period of about 100 000 years; (2) changes in Earth's obliquity between 22.1° and 24.5° with a period of about 41 000 years; and (3) lunisolar precession with a period of 25 771.5 years. Furthermore, the orientation of Earth's orbit in space is slowly changing. This movement is called apsidal precession and, combined with the lunisolar or axial precession, alters the 25 771.5 years period to an average of 23 000 years on average (varying between 20 800 and 29 000 years). In reality, these astronomical mechanisms are considerably more complex but well known, and the effects of the different mechanisms on climate deviate partly from those expected. In addition, the aforementioned periodicities are not constant throughout Earth's history, because of the evolution of the Earth–Moon system (e.g., Meyers and Malinverno, 2018). The Milankovitch theory, its modern development and critique, as well as the subdivision of ice ages into glaciations and interglaciations is treated in more detail in Section 5.1. The primary aim of Section 5.1. is to clearly distinguish the concept of ice ages from that of glaciations and interglaciations. The fourth type of model described by Walzer and Hendel (2022) is stratigraphic models, which are key in determining the onset and termination of an ice age (e.g., the Sturtian and Marinoan). Hoffman et al. (2017) reported that the Sturtian onset, Sturtian termination, and Marinoan termination were *globally synchronous*, as inferred by combined U–Pb and Re–Os dating. Multiple cap carbonates of different ages have not been found. Therefore, the terminal deglaciations of ice ages were unique events. The stratigraphy allows the following time intervals to be defined.

Table 1
Cryogenian glaciations

Marinoan deglaciation	:	636.0 to 634.7 Ma	635 Ma
Marinoan onset	:	649.9 to 639.0 Ma	646 ± 5 Ma
Sturtian deglaciation	:	659.3 to 658.5 Ma	661 Ma
Sturtian onset	:	717.5 to 716.3 Ma	717 Ma

The first and second columns of numbers are ages for all continents according to Hoffman et al. (2017). The third column of numbers refers to Cryogenian sediments in NW Namibia according to Hoffman et al. (2021). In addition to the small list, it should be noted that according to Macdonald et al. (2010) 716.5 Ma are to be assumed as a minimum age constraint on Sturtian snowball onset because it took ≤400 ka after snowball onset for ice sheets to thicken and flow, producing evidence of glacial action at sea level as observed by those authors. 663.03±0.11 Ma (Cox et al., 2018) dates Sturtian deglaciation on the assumption that the Willyerpa Formation is syndeglacial in origin. We use the Neoproterozoic chronology shown in Fig. 1 of Rooney et al. (2015). Rooney et al. (2015) presented Re–Os geochronological constraints on the Sturtian onset and deglaciation, and Marinoan termination on three different paleocontinents. Fig. 5 is a compilation and combines the Re–Os ages of Rooney et al. (2015) with other Re–Os and igneous U–Pb age constraints. No detrital zircon U–Pb ages are included, as these cannot constrain the beginning or termination of an ice age. For our graphic presentation, we use an age for the Sturtian ice age of 717.4–659.6 Ma and for the Marinoan ice age of 640.7–635.5 Ma. In this context we would like to refer to the high-quality U–Pb (CA-ID-TIMS) data on cap carbonates in Zhou et al. (2019).

It is difficult to establish a robust stratigraphic model for the Paleoproterozoic glacial epochs. Hoffman (2013) proposed a scheme that involves only three such epochs, in North America, southern Africa, and Western Australia. Tang and Chen (2013) presented a comprehensive compilation of lithostratigraphic and geochronological data for the Paleoproterozoic ice ages (Fig. 6). Glacial diamictites can be used to subdivide a small percentage of the Paleoproterozoic in North America into 3–4 ice ages, but on other continents only one diamictite unit is present, possibly due to erosion. There were certainly two, to be precise Duitschland and Rietfontein, and perhaps three (Makganyene) Paleoproterozoic glaciations on Kaapvaal craton, South Africa. The only Paleoproterozoic glacial formation surely known to have been deposited a low paleolatitude is the ca 2.43-Ga Makganyene glaciation (Evans et al., 1997). Therefore, it is also referred to by Kopp et al. (2005) as Makganyene snowball Earth. The Rietfontein (Boshhoek) glaciation occurred at high paleolatitude according to new paleomagnetic data.

Tang and Chen (2013) also concluded that Paleoproterozoic ice ages were synchronous worldwide. A detailed stratigraphic model of Paleoproterozoic supracrustal rocks on the northern coast of Lake Huron has been constructed by Young (2013). Caqueneau et al. (2018) investigated the zircon U–Pb geochronology of the early Proterozoic Turee Creek Group, Hamersley Basin, Western Australia. This siliciclastic-dominated sedimentary sequence contains at least two diamictitic units with similarities to other Paleoproterozoic glacial sediments from South Africa and North America (Lake Huron). However, to some extent, the correlation of these ice ages is ambiguous. Fig. 7 shows a possible correlation of these ice ages. Even if we combine the two glacial diamictite horizons in the Gowganda Formation (cf. Figs. 6 and 7) into one glacial epoch, Fig. 7 suggests there were four Paleoproterozoic ice ages, which is in broad agreement with the results of Hoffman (2013) (see his Fig. 1), although Hoffman (2013) suggested there were only three Paleoproterozoic ice ages. Estimations of onsets and terminations for these Paleoproterozoic ice ages are as follows:

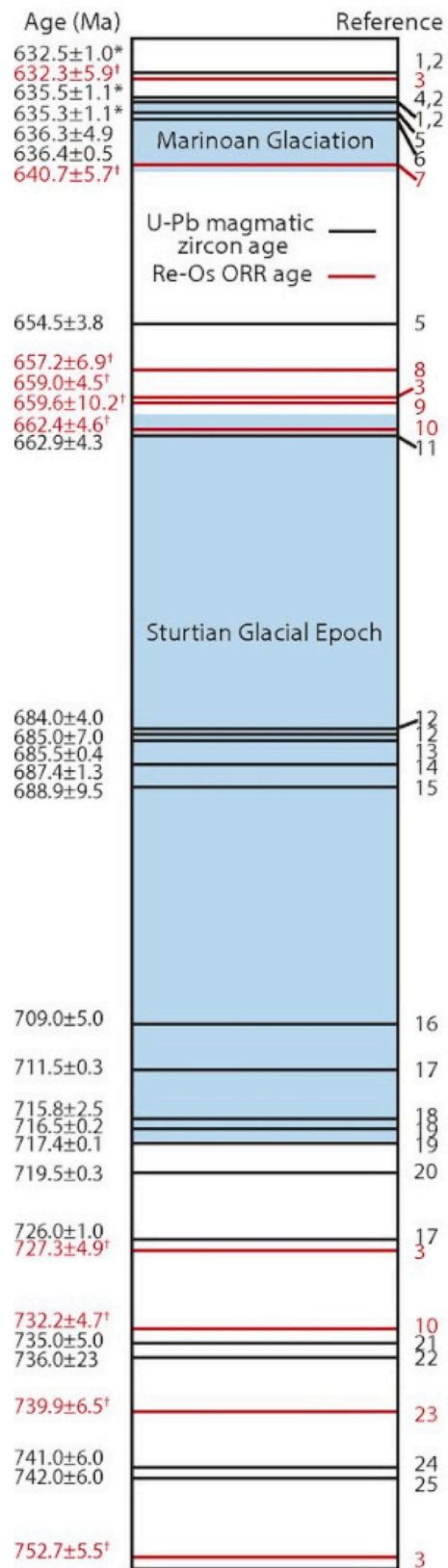


Fig. 5. Geochronological constraints on the Sturtian and Marinoan ice ages, based on Rooney et al. (2015).

Table 2
Paleoproterozoic glaciations

Rietfontein glaciation onset	:	2250 Ma; termination: 2240 Ma
Gowganda glaciation onset	:	2340 Ma; termination: 2310 Ma
Bruce glaciation onset	:	2410 Ma; termination: 2384 Ma
Ramsay Lake glaciation onset	:	2460 Ma; termination: 2435 Ma

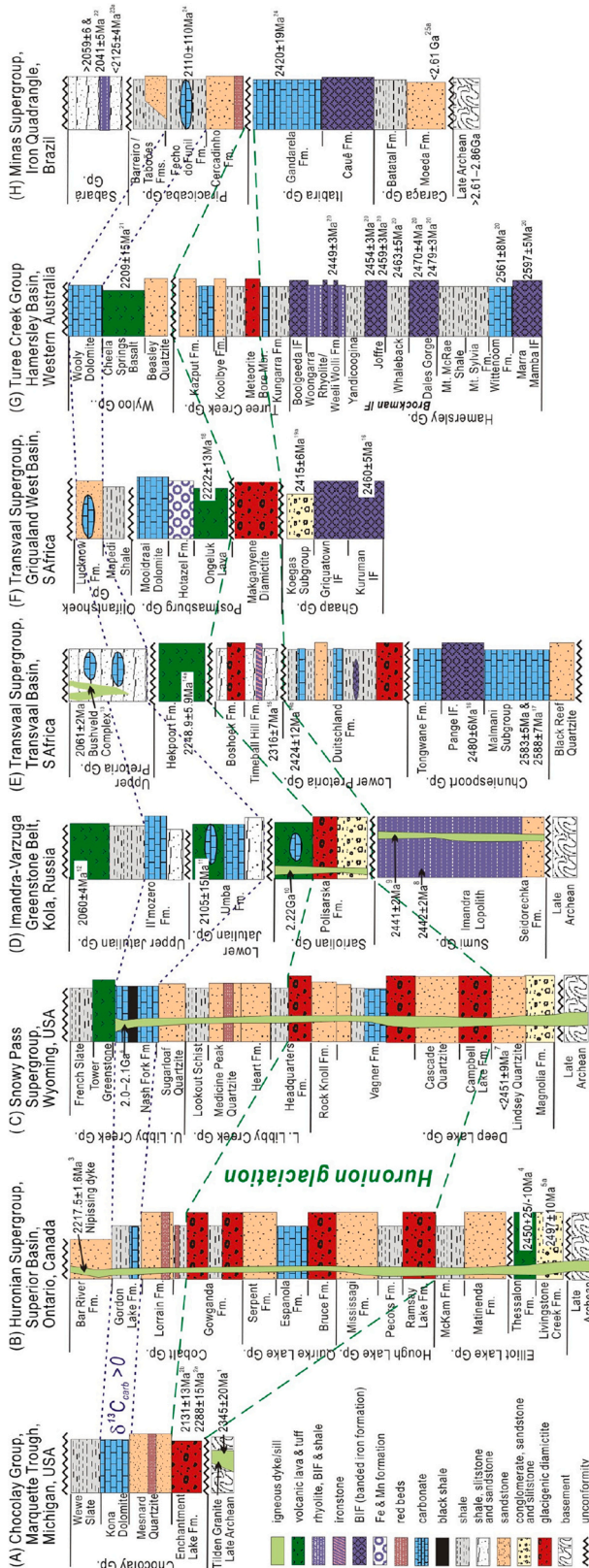


Fig. 6. Stratigraphic correlations of early Paleoproterozoic glaciations, based on Tang and Chen (2013) and references therein.

Although these ages have uncertainties, they are needed to construct Figs. 1–4. These estimated values are from a combination of results from Caquineau et al. (2018) and Tang and Chen (2013). However, our final conclusions are independent of the exact ages. Gumsley et al. (2017) identified four Paleoproterozoic ice ages (cf. Fig. 14), in agreement with Rasmussen et al. (2013) and Schröder et al. (2016), with the fourth ice age occurring during $\leq 2250\text{--}2240\text{ Ma}$. Notably, there is no record of continental ice sheets at any paleolatitudes between 2.22 and 0.75 Ga (Hoffman, 2009), which is consistent with Stern and Miller (2019), see their Fig. 1. Between the Rietfontein glaciation termination and Sturtian snowball Earth onset, there is a 1522.5 Ma gap with no glaciation. This was already known to Hoffman and Schrag (2002). However, this has not been widely considered in the numerous hypotheses proposed to explain the occurrence of the major glaciations. Here, we omit the compilation of onsets and terminations of the other ice ages, which is necessary to construct Figs. 1–4.

Hoffman et al. (2017) reported that the Sturtian onset and termination were globally synchronous, based on U–Pb and Re–Os dating. Cap carbonates and post-glacial ocean stratification after the Sturtian and Marinoan glaciations exhibited similar rapid changes with big resemblance. Crockford et al. (2018) propose that rapid dissipation of the sulfate $\Delta^{17}\text{O}$ anomaly produced by stratospheric photochemistry on snowball Earth provides a tighter constraint on synchronicity and duration of Marinoan deglaciation than is possible with any existing radiometric method. Cap carbonates sharply overlie sediments deposited in both Cryogenian ice ages and are globally distributed (James et al., 2001; Jiang et al., 2006; Hoffman et al., 2007; Hoffman et al., 2017). Cox et al. (2018) also noted the global similarity in the timing of the Sturtian termination. Wang et al. (2020) use high-resolution stratigraphic profiles of the chemical index of alteration (CIA) and show that the CIA can serve as a robust proxy for a rapid increase in chemical weathering intensity. Thus, using the example of the Sturtian termination in southern China, it was shown that the climate transition at the end of an ice age is relatively fast also in this case. We present Fig. 8 to show that it is insufficient to explain only the temporal distribution of the ice ages. It is important to understand why the onsets and terminations are relatively fast and why the ice ages have a duration of millions of years. Rapid onsets and terminations at low paleolatitudes is an intrinsic property of the ice-albedo bifurcation. Synchronous, as distinct from rapid, deglaciation at all latitudes is intrinsic to the CO_2 hysteresis required to trigger snowball deglaciation. As these are corollaries of snowball states, they constitute tests of their occurrence.

The termination of the Cryogenian snowball Earth periods is evidently caused by the accumulation of volcanic carbon dioxide in the atmosphere (Hoffman et al., 1998). The period following the glaciation has high atmospheric temperatures and an increased silicate weathering. West et al. (2005) showed, however, that the availability of fresh silicate rocks is a limiting factor for silicate weathering. Mills et al. (2011) developed a model in which this transport-determined limitation is built into the COPSE model. The resulting new model generates greenhouse-icehouse oscillations that are compatible with the geological observation. Fig. 8 shows for two successive glaciations that the temperature increase is strongly nonlinear. The nonlinear temperature rise means that a small difference in the Earth’s albedo results in a large difference in snowball Earth duration.

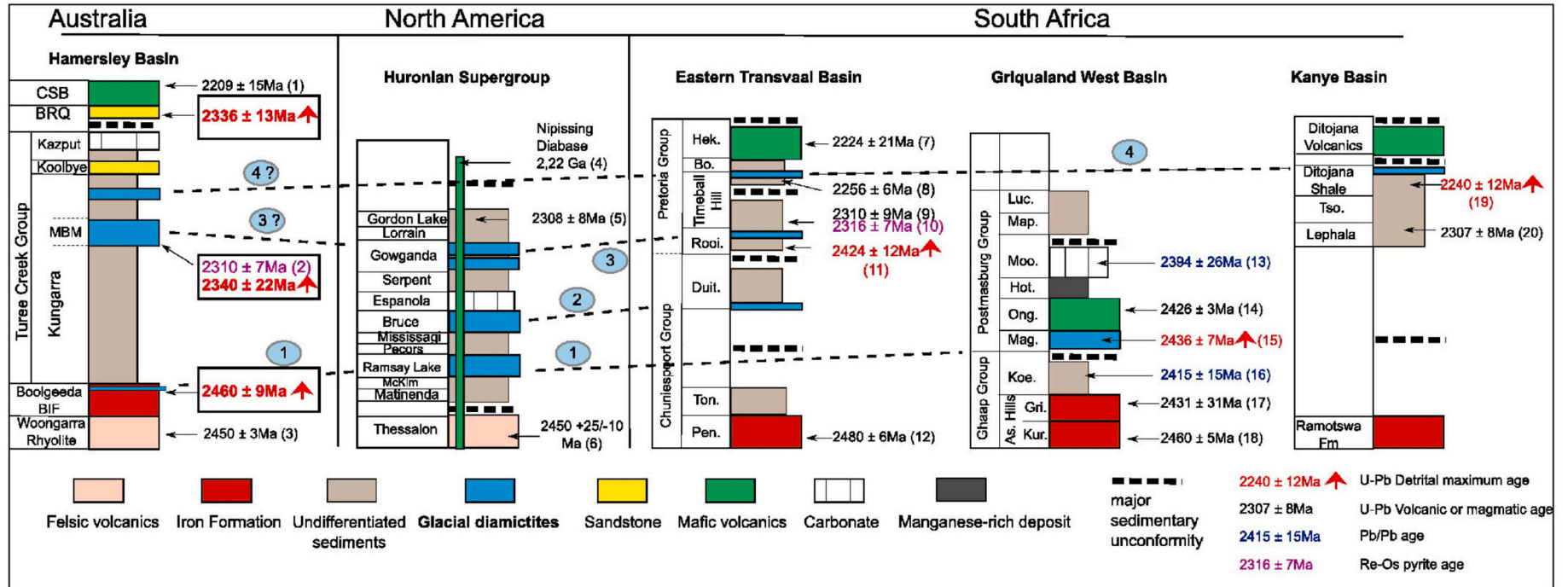


Fig. 7. Stratigraphic model of early Paleoproterozoic glaciations in Western Australia, North America, and South Africa, based on Caquineau et al. (2018). Abbreviations: BRQ = Beasley River Quartzite; CSB = Cheela Springs Basalt; Pen. = Penge Iron Formation; Ton. = Tongwane Formation; Duit. = Deutschland Formation; Rooi. = Rooihooigte Formation; Bo. = Boshhoek Formation; Hek. = Hekpoort Formation; Kur. = Kuruman Iron Formation; Gri. = Griqualand Iron Formation; Koe. = Koegas subgroup; Mag. = Makganyene Formation; Ong. = Ongeluk Volcanics; Hot. = Hotazel Formation; Moo. = Mooidraai Dolomite; Map. = Mapedi Shale; Luc. = Lucknow Formation; Tso. = Tsokwane Quartzite.

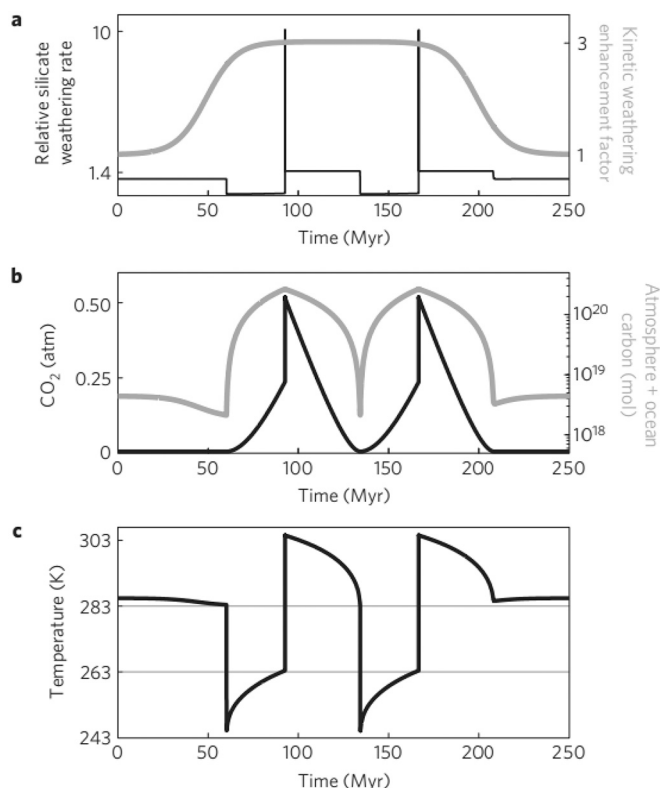


Fig. 8. For the presented two successive glaciations, the temperature rise is strongly nonlinear. According to Mills et al. (2011), this picture shows a cyclic solution when the steady-state temperature is forced below the ice-albedo runaway value for 150 Ma. a: The imposed kinetic weathering enhancement is shown in grey; in black is the weathering rate relative to present. b: Total atmosphere and ocean carbon (grey) and atmospheric carbon dioxide (black). c: Temperature (solid line) alongside snowball entry and exit thresholds (thin grey lines).

4. Do the onsets and terminations of the Sturtian and Marinoan glaciations occur relatively quickly or do they require a few million years each?

There are strongly divergent views on the speed of deglaciation after a snowball Earth epoch. Hir et al. (2009) develop a hierarchy of numerical models of the snowball Earth aftermath. These models show that the hydrological cycle intensifies only weakly in response to the elevated greenhouse. Their main conclusion is that “postglacial silicate weathering was likely not as vigorous as commonly assumed (Higgins and Schrag, 2003; Hoffman et al., 2007)”. Furthermore, Hir et al. (2009) conclude that “the time required to restore CO₂ concentrations to roughly pre-glacial levels is on the order of a few million years, rather than a few thousand years, as has been previously assumed (Higgins and Schrag, 2003)”. The simulations in Hir et al. (2009) were intended to estimate the timescale for silicate weathering to provide the alkalinity flux for cap carbonate production. Hoffman et al. (1998), Higgins and Schrag (2003), and Hoffman et al. (2007) had assumed a sufficient alkalinity flux on a timescale of millennia which corresponds to the deglaciation timescale, whereas Hir et al. (2009) estimated it would take from 10⁵ up to a few million years. The problem with Le Hir’s et al. (2009) simulation is that it neglected carbonate weathering, which is a much faster process than silicate weathering (Higgins and Schrag, 2003). It also did not consider the effect of ocean warming on carbonate saturation (Fabre et al., 2013) nor the alkalinity already present in the ocean as a result of millions of years of buffering seawater acidification through carbonate dissolution and sea-floor weathering (Higgins and Schrag, 2003). Hoffman et al. (2007) demonstrated isotopically that a

Marinoan cap dolomite in Namibia was deposited diachronously during progressive flooding of an ancient continental slope and shelf having 400–600 m of paleotopographic relief, thereby linking cap dolomite sedimentation in time with large-magnitude sea-level rise associated with global ice-sheet meltdown. Ice-sheet meltdown cannot be a slow process, because of ice-albedo and ice-elevation feedbacks. Consider that mid-latitude glaciers in the European Alps have been lowered at an average rate of 1.6 m per year over the past 50 years (Vincent et al., 2017). At this rate, virtually all snowball ice sheets would disappear in 3–5 ka. This should be a maximum duration since most snowball ice sheets were closer to the equator and to sea-level than Alpine glaciers, and CO₂ levels were ~100 times higher. The vast majority of Marinoan cap dolomites worldwide have sharp bases and gradational tops, passing upward into deeper-water facies. They extend over wide areas and paleotopography, forming the transgressive systems tracts of typically expanded depositional sequences. Basic stratigraphic relations make it difficult not to associate transgressive cap dolostone with the ice sheet meltdown millennial timescale and the whole-ocean warming decamillennial timescale. A short timescale for Marinoan cap dolostones is supported by the sulfate $\Delta^{17}\text{O}$ anomaly in seafloor barite at the tops of cap dolomites in several areas (Crockford et al., 2018; Crockford et al., 2019).

However, Hir et al. (2009) conclude from model simulations that it takes millions of years for the silicate weathering cycle to obtain the necessary post-snowball CO₂ level. Based on their 3D-climate model, they conclude that the transition cannot be vigorous. The result of Hir et al. (2009) is caused by the fact that the relationship between average continental temperatures and runoff rates under very high CO₂ levels are nonlinear. For example, for a 400 PAL CO₂ climate, the computed discharge of dissolved elements from continental weathering into the ocean is slightly less than a 10-fold increase in comparison to the present-day value. The abbreviation PAL means present atmospheric level. Le Hir’s et al. (2009) conclusion is indirectly supported by Rooney et al. (2020). The latter find that the apparent diachroneity of the Sturtian deglaciation can be explained as a consequence of stratigraphic condensation. Font et al. (2010), on the other hand, are more oriented to the geological observational facts and present detailed magnetostratigraphic data of the Mirassol d’Oeste cap dolostones and compiled data from other post-Marinoan outcrops. They conclude that the duration of the Marinoan deglaciation is 10 ka - 100 ka, because they equate this with the time span of the deposition of the Marinoan dolostones.

With regard to the previous paragraph, the following must be noted: Le Hir’s et al. (2009) point about the nonlinear relationship between CO₂ and the hydrologic cycle is correct, but there are other aspects. The intensity of post-snowball carbonate dissolution and silicate weathering was not solely due to the greenhouse climate, but rather to the mantle of highly-reactive fresh rock powder, i.e. loess, and unweathered till, exposed by global ice-sheet retreat, as well as little-weathered volcanic products accumulated over millions of years under ice (Hoffman and Schrag, 2002; Fabre and Berger, 2012). Diachroneity of Sturtian cap carbonates is not relevant to the duration of Marinoan cap dolomites. Sturtian cap carbonate sequences, including South China, generally lack transgressive tracts, i.e. cap dolomites *sensu stricto*. This appears to reflect a combination of deeper subsidence (longer-lived snowball) and delayed onset of carbonate production until after major sea-level rise was completed.

The argument of Font et al. (2010) depends on an actualistic assumption of reversal frequency. If geomagnetic field intensity was significantly less than present, as it was in during intervals of the Ediacaran, Cambrian and Devonian, there is no constraint on the frequency and speed of geomagnetic reversals, only on the sedimentation rates capable of recording them. The highly aggradational character of sedimentary structures within Marinoan cap dolomites, e.g., tubestone stromatolite and giant wave ripples, as well as crystal-fans (seafloor cement) in directly overlying deeper-water limestone imply rapid

accumulation and anomalous carbonate oversaturation, supported by the anomalous poleward extent of Marinoan cap dolomites (Hoffman and Li, 2009) compared with nonskeletal carbonate distribution over geologic time (Opdyke and Wilkinson, 1990).

We first give an uncommented literature review here. Only afterwards do we evaluate individual papers. McMenamin (2004) explains onset and termination of the two Cryogenian glaciations by the influence of the biosphere. Massive growth of giant stromatolites and major blooms of phytoplankton produced large drops of atmospheric carbon dioxide and thereby the abrupt onset of a snowball Earth. Subsequently, however, cryoconites and hyperscums developed during the Cryogenian glaciations, which supposedly can explain the rapidity of deglaciation. Myrow et al. (2018) study wave ripples and tidal laminae in the Elatina Formation (Australia) that developed after the Marinoan glaciation. They found that water depths of 9 to 16 meters remained nearly constant for about 100 years and 27 meters of sediment. This high accumulation rate cannot be explained by subsidence, but by a very rapid rate of sea level rise, i.e. 0.2 to 0.27 m/a. From this, Myrow et al. (2018) conclude a very rapid deglaciation. - Lang et al. (2018) study pyrite concretions that lie immediately beneath the cap carbonate. The associated sedimentary sequence belongs to the termination of the Marinoan glaciation in the Yangtze Block (China). Ocean models calculated in conjunction show that the ocean experienced a rapid increase in pH and physical stratification, followed by a rapid oceanic overturn. Lang et al. (2018) propose a transient presence of marine euxenia in an ocean with redox stratification and high bioproductivity. - Zhou et al. (2019) publish new high-precision U-Pb zircon ages that argue for a rapid termination of the Marinoan glaciation. In any case, they suggest that the duration of the cap dolostone was considerably less than 10^6 years. A compilation of worldwide data shows that the new data are consistent with a global synchronicity of Cryogenic deglaciation events. - Nordsvan et al. (2019) examine a combination of paleomagnetic, sequence-stratigraphic, and sedimentological data and conclude rapid deglaciation with protracted cap dolostone precipitation. They emphasize that the duration of cap dolostone accumulation is not directly linked to the time scale of snowball Earth deglaciation. Usually, cap dolostone units are interpreted as transgressive deposits with some magnetic reversals. Usually it is concluded that they were accumulated in more than 10^5 years. This conclusion is contradicted by Nordsvan et al. (2019), who propose that cap dolostones represent sediment starvation following a major landward coastal migration caused by the deglaciation of the thick snowball Earth ice sheet. - Yu et al. (2020) address several hypotheses regarding carbonate formation and conclude that cap carbonates were formed by a combination of inorganic-chemical and microbial processes in a stratified ocean with a low-salinity lid. Ramme and Marotzke (2022) apply a coupled atmosphere–ocean circulation model (AOGCM). Their simulations show that the freshwater stratification break down on a time scale of about 10^3 years. This conclusion is almost independent of the CO_2 scenario used. The thermal expansion of seawater causes a sea level rise of only 8 meters during 3000 years. This is roughly consistent with the observations of Myrow et al. (2018).

Here are some comments to the last paragraph. Nordsvan et al. (2019) ignore the shallow-marine origin and transgressive nature of most Marinoan cap dolomites. - The postglacial destratification timescale, i.e., mixing between the cold dense residual brine and a low-density meltwater lid, provides a valuable constraint on the timescale of Marinoan cap dolomite deposition. Seafloor barite (BaSO_4), which occurs at the top of cap dolomites on different paleocontinents, implies mixing between two distinct aqueous reservoirs, one rich in sulfate and the other in Ba. These ions cannot coexist in solution in significant concentration because of the extreme insolubility of barite. Crockford et al. (2016), Crockford et al. (2018) demonstrated that the sulfate in cap barite was borne by the meltwater lid, since it carries the $\Delta^{17}\text{O}$ anomaly of atmospheric O_2 , transferred to sulfate during oxidative weathering of sulfide-bearing rocks. Crockford et al. (2019) showed that the Ba came from the anoxic and well-mixed snowball brine, since its Ba-isotopic

composition is globally uniform and indistinguishable from modern pelagic barite. Brine-meltwater mixing has also been inferred from Sr and O-isotopes in Marinoan cap dolomite itself. Estimated destratification timescales on the order of 40–60 ka (Yang et al., 2017) or a thousand years (Ramme and Marotzke, 2022), as constraints on cap dolomite deposition, are incompatible with the 10^5 – 10^6 years estimates of Font et al. (2010) and Nordsvan et al. (2019), the former based on paleomagnetic reversals. The rate of sea-level rise estimated by Ramme and Marotzke (2022), 8 m in 3000 years, is 100 times slower than Myrow's et al. (2018) estimate of 0.2–0.27 m/a. Yang et al. (2017) and Ramme and Marotzke (2022) simulated the ocean destratification timescale differently. Given the importance of continental margins in vertical ocean mixing, it is not surprising that the 1-D model (Yang et al., 2017) destratified more slowly, but quantitative comparison is made difficult by differences in boundary conditions. The prescribed sea-glacier thickness may be critical because it melts first and most rapidly, being in warmer air and bathed in water. Yang et al. (2017) prescribe a km-thick sea-glacier whereas its thickness in Ramme and Marotzke (2022) is limited to ≤ 30 m by the duration of the pre-deglacial model run. Both prescriptions as rather extreme, in opposite directions, and perhaps the truth lies between their respective estimates. The important point is that both estimates point to a short timescale for deposition of Marinoan cap dolomite.

Hoffman et al. (2017) find that uranium-lead and rhenium-osmium age determinations show that the onset of Sturtian glaciation and the terminations of Sturtian and Marinoan glaciations are globally synchronous. Furthermore, their Table 1 shows that the onset and termination were “sharply defined in time.” For example, the onset of the Sturtian cryochron at low ($21^\circ \pm 3^\circ\text{N}$) paleolatitude is constrained by U-Pb zircon ages between 717.5 and 716.3 Ma. The Sturtian termination is constrained between 659.3 and 658.5 Ma. Hoffman et al. (2021) publish similar ages for NW Namibia and conclude that each glaciation began and ended abruptly. However, as shown above, the probably correct time intervals for onset or termination of a glaciation are considerably shorter than it seems when considering only the radioactive age determinations just mentioned. Hoffman used the term “abrupt” to describe Cryogenian glacial onsets and terminations based on physical stratigraphic expression, before any direct radiometric age constraints existed. The implication was that glaciation and deglaciation were unidirectional and rapid at the regional scale. It was not meant to imply synchronicity between regions. Glacial onsets are commonly marked by an erosive contact, making their abruptness less significant than for terminations, where contacts are typically non-erosive. Cryogenian deglaciations were likely to be faster than Quaternary deglaciation because nearly all Cryogenian ice sheets were at lower latitude and p_{CO_2} was about a hundred times higher. The total energy required for melting is large but not limiting, ~ 5 – 6 W m^{-2} averaged over 2 ka. Over 200 W m^{-2} was available, even with 6–7% lower solar luminosity at that time. The snowball glacial-deglacial cycle can be viewed as the interaction between climate feedbacks operating on different timescales: positive ice-albedo and ice-elevation feedbacks operating on a timescale of months, and silicate-weathering feedback operating on a timescale of millions of years. The former govern the onsets and terminations, while the latter governs the time elapsed between them.

5. Natural climate change: faster changes

5.1. Glacial–interglacial cycles: the Earth system is not isolated

It may be instructive to examine the subdivision of glaciations into glacial and interglacial. Milankovitch (1941) showed that variations in the eccentricity of Earth's orbit, obliquity, and precession generate changes the distribution of the solar radiation energy reaching Earth over the different seasons of the year. The Milankovitch (1941) theory is based on the supposition that glaciers and ice sheets grow when

summers are cool and short at $\sim 65^\circ\text{N}$, e.g. at the Laurentide and Scandinavian ice-sheet centres. This is because their growth depends on the survival of some fraction of winter snowfall through the summer melting season. Already before, Milanković (1920) wrote that the prerequisite for ice cover to form and then extend over the Earth are cool summers, although the winters may be relatively mild. Milankovitch's (1941) theory was first supported by spectral analysis of deepsea sediment $\delta^{18}\text{O}$ records (Hays et al., 1976). These were confirmed a decade and a half later by polar ice-core $\delta^{18}\text{O}$ records, covering much shorter timescales but with additional proxies, i.e. δD , trapped CO_2 , CH_4 , dust content, etc., and higher resolution. Fig. 9 presents an application of this theory from Petit et al. (1999). The lower curve of Fig. 9 shows the computed mid-June insolation at 65°N (in $\text{W} \cdot \text{m}^{-2}$). Fig. 9 also shows measured data from ice cores from Antarctica. Spectral analysis of the measured data yields periods of 100, 41, 24, and 19 ka (1 ka = thousand years). This appears to be consistent with the Milankovitch theory, although one might initially suspect that Antarctica is not necessarily representative of the whole Earth. However, Lisiecki and Raymo (2005) published a 5.3-Ma stack of benthic $\delta^{18}\text{O}$ records from 57 globally distributed sites, which were aligned with an automated correlation algorithm. The atmospheric CO_2 , temperature, and CH_4 curves in Fig. 9 (Petit et al. (revised January 2000)) agree well with the $\delta^{18}\text{O}$ curve of Lisiecki and Raymo (2005). In addition, Strunk et al. (2017) investigated the climate and modeled the glacial history of Greenland in the last 1 Ma (Fig. 10). They quantified the exposure and denudation history using paired cosmogenic ^{10}Be - ^{26}Al bedrock data. Furthermore, El'gygytyn (Siberia) diatom productivity (Si/Ti) data can also be considered a proxy for temperature (Melles et al., 2012). This proxy is consistent with the LR04 benthic $\delta^{18}\text{O}$ curve of Lisiecki and Raymo (2005). Therefore, we

conclude that the Vostok ice core time-series in Fig. 9 is a proxy for the global climate of the past 400 ka.

However, three *real* problems are evident in Figs. 9 and 10. Kaufmann and Juselius (2016) noted that the insolation signal produced by eccentricity is only about 2 W/m^2 , whereas accumulation and ablation of ice exhibits a strong 100 ka cycle signal. The insolation signal from precession is about 100 W/m^2 , and that from obliquity is 20 W/m^2 . As such, the *first* problem is the nature of the *amplification effect* for the 100 ka cycle or an alternative forcing mechanism. Only a minority of researchers propose the second alternative. For example, Arnaut and Ibáñez (2020) presented a conceptual model, whereby the oscillations are produced by photosynthesis and the carbon cycle. A *second* problem often considered is the following: The lowermost curve of Fig. 9 is a superposition of only a few sine curves. However, the upper curves of Fig. 9 and all curves of Fig. 10 exhibit a distinctive saw-tooth pattern. The 5.3 Ma stack of benthic $\delta^{18}\text{O}$ records (Lisiecki and Raymo, 2005) and similar observations reveal a *third* hitherto unresolved problem, which is the dominance of the 100 ka cycle and saw-tooth pattern in the youngest time interval (Fig. 10), whereas the 41 ka cycle formerly prevailed. The *temporal boundary* between the two intervals cannot be determined exactly. It is located between 1000 ka and the Brunhes–Matuyama reversal of the geomagnetic dipole (i.e., 781 ka), which was the last reversal of Earth's magnetic dipole field.

Lisiecki (2010) undertook statistical analyses of insolation and climate of the past 5 Ma, and found that the time-dependent 100 ka power of eccentricity is anti-correlated with the mean temperature of climate. A strong eccentricity forcing is associated with a weaker power in the 100 ka glacial cycle. It was suggested that internally driven climate feedbacks cause the 100 ka climate variation. The following papers are focused on similar ideas. Rial et al. (2013) explained the first

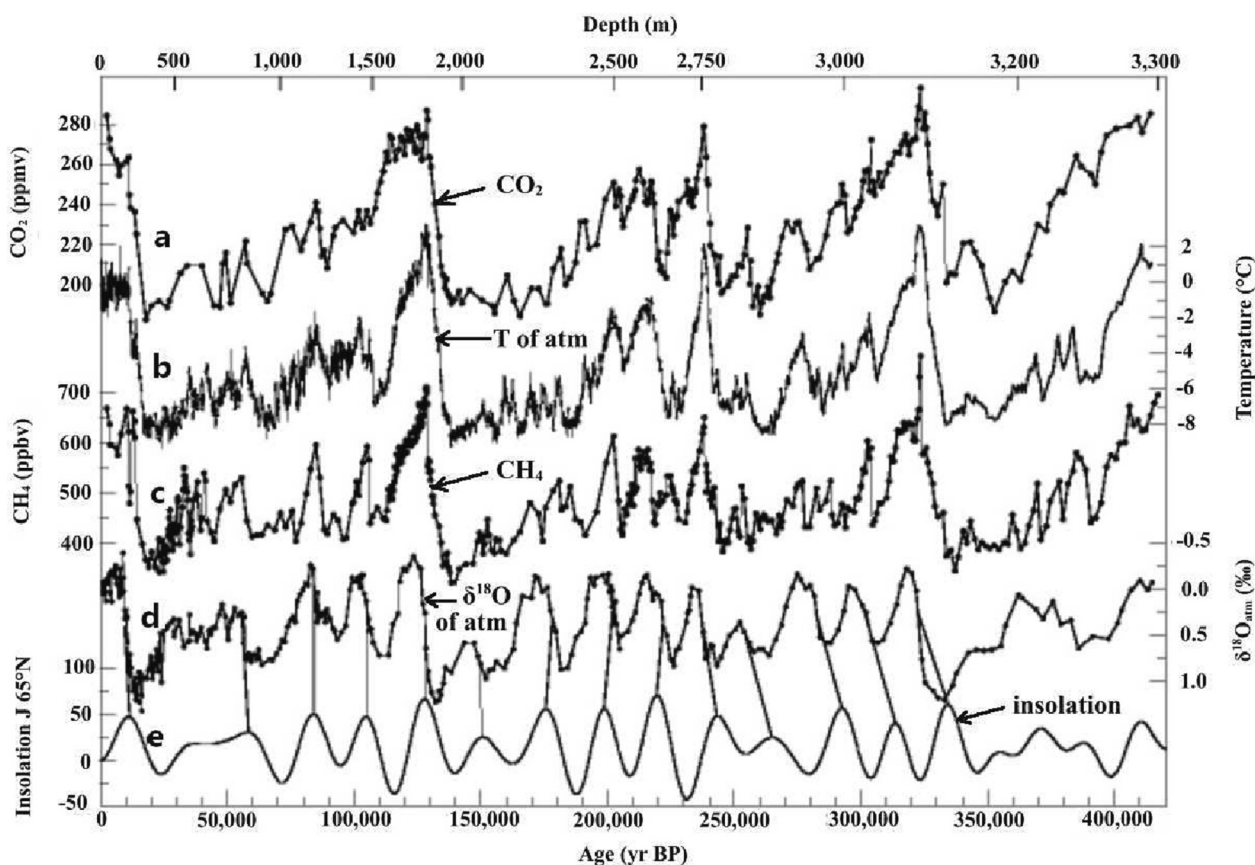


Fig. 9. Time-series of measurements taken from the Vostok ice core, Antarctica, based on Petit et al. (1999), and compared with mid-June insolation at 65°N (in $\text{W} \cdot \text{m}^{-2}$) (Berger, 1978). The lower axis is the GT4 age and the corresponding depths are shown on the upper axis. (a) CO_2 ; (b) atmospheric temperature; (c) CH_4 ; (d) atmospheric $\delta^{18}\text{O}$; (e) incoming insolation.

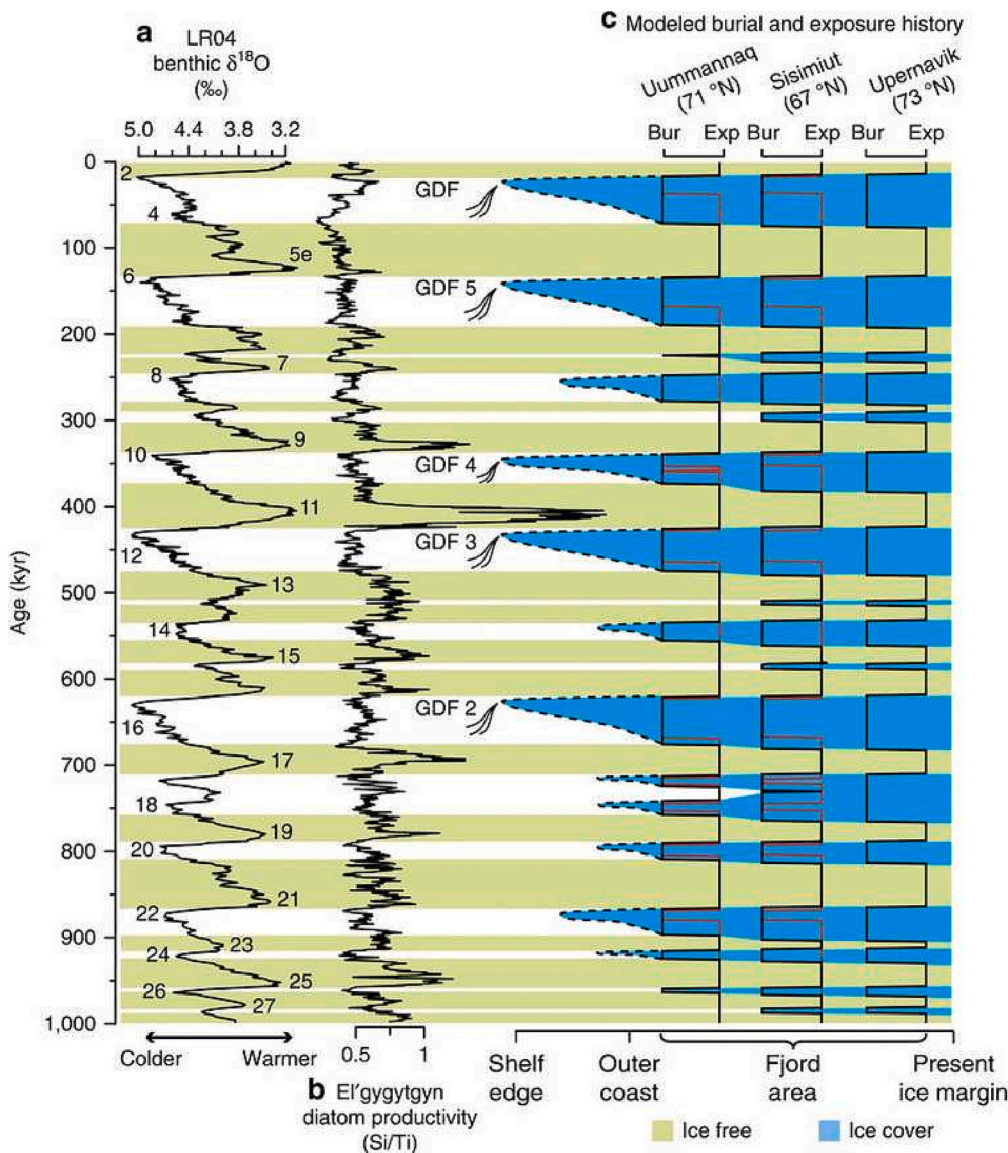


Fig. 10. Glacials and interglacials in west Greenland, based on [Strunk et al. \(2017\)](#). Curve a on the left-hand side is a 1000 ka segment of the 5.3 Ma stack of benthic $\delta^{18}\text{O}$ records from 57 globally distributed sites from [Lisiecki and Raymo \(2005\)](#). The $\delta^{18}\text{O}$ curve represents the global ice volume. The numbers refer to marine isotope stages. Curve b is the diatom productivity record of Lake El'gygytyn (east Siberia) from [Melles et al. \(2012\)](#), which is a temperature proxy. Curves c show exposure (Exp) and burial (Bur) by ice cover at three sites near the coast of west Greenland. The black lines are based on 39 bedrock samples. Red lines denote the glaciation history of samples with very short burial durations. Glacials are represented in blue, and interglacials in green. This figure shows that the continuing alternation of glacials and interglacials is a global phenomenon and, furthermore, that the saw-tooth pattern has persisted for the last 1000 ka.

problem by the synchronization of nonlinear internal climate oscillations and the 413 ka eccentricity cycle. They used spectral analysis to show that the climate system first synchronized to the 413 ka eccentricity cycle at 1.2 Ma and has remained synchronized since that time. The synchronization generates a nonlinear transfer of energy and frequency modulation that increases the amplitude of the 100 ka cycle. These results are consistent with the multivariate approach of [Kaufmann and Juselius \(2016\)](#). The latter advocated a weaker form of the Milankovitch hypothesis, whereby internal climate dynamics impose perturbations on glacial cycles that are driven by solar insolation. The results show that a slow response exists between land ice volume and solar insolation. [Abe-Ouchi et al. \(2013\)](#) presented a comprehensive climate and ice sheet model to explain the 100 ka cycle, where the lithosphere–asthenosphere system plays an important role. Although CO_2 is involved, it is not the main control on the 100 ka cycle. As such, the saw-tooth problem has evidently been solved and the calculated spectra of ice volume changes show a predictable distribution of peaks. [Huybers \(2011\)](#) showed that both obliquity and precession control late Pleistocene glacial cycles. [Huybers et al. \(2019\)](#) concluded that glacial cycles were controlled by Northern Hemisphere summer insolation during the late Pliocene and entirety of the Pleistocene, which supported the Milankovitch theory of orbital control on the timing of glacials and

interglacials. We do not want to conceal a *fourth* problem that many previous studies do not mention: [Laskar et al. \(2011\)](#) presented an accurate orbital solution for the long-term motion of Earth. The precession equations were revised. The spin of the Earth is affected by the tidal torque of the Moon. [Laskar \(2019\)](#) suggested that uncertainties in the tidal dissipation over time affect the accuracy of the precession solution beyond 20 Ma.

In the previous Sections on the slow parts of natural climate change, we have seen that the corresponding mechanisms are closely linked with the evolution of atmospheric concentrations of carbon dioxide and methane. Therefore, it is also of interest to see how these quantities behave with respect to faster changes. [Fig. 11](#) is noteworthy because it shows that the changes in atmospheric concentration of CO_2 and NH_4 is closely tied to the temperature curve, because $\delta^{18}\text{O}$ is a reciprocal measure of temperature. However, it is not clear from the curves whether the increase in carbon dioxide causes the temperature increase or vice versa. [Fig. 11](#) is shown because the history of the temperature and the CO_2 concentration of the Huroic and Cryogenic atmospheres is not known at this large temporal resolution. Two important conclusions can be drawn from this Section on glacials and interglacials. First, atmospheric carbon dioxide may not always be the driving force of natural climate change. Second, climate change *on this scale* is driven, first, by

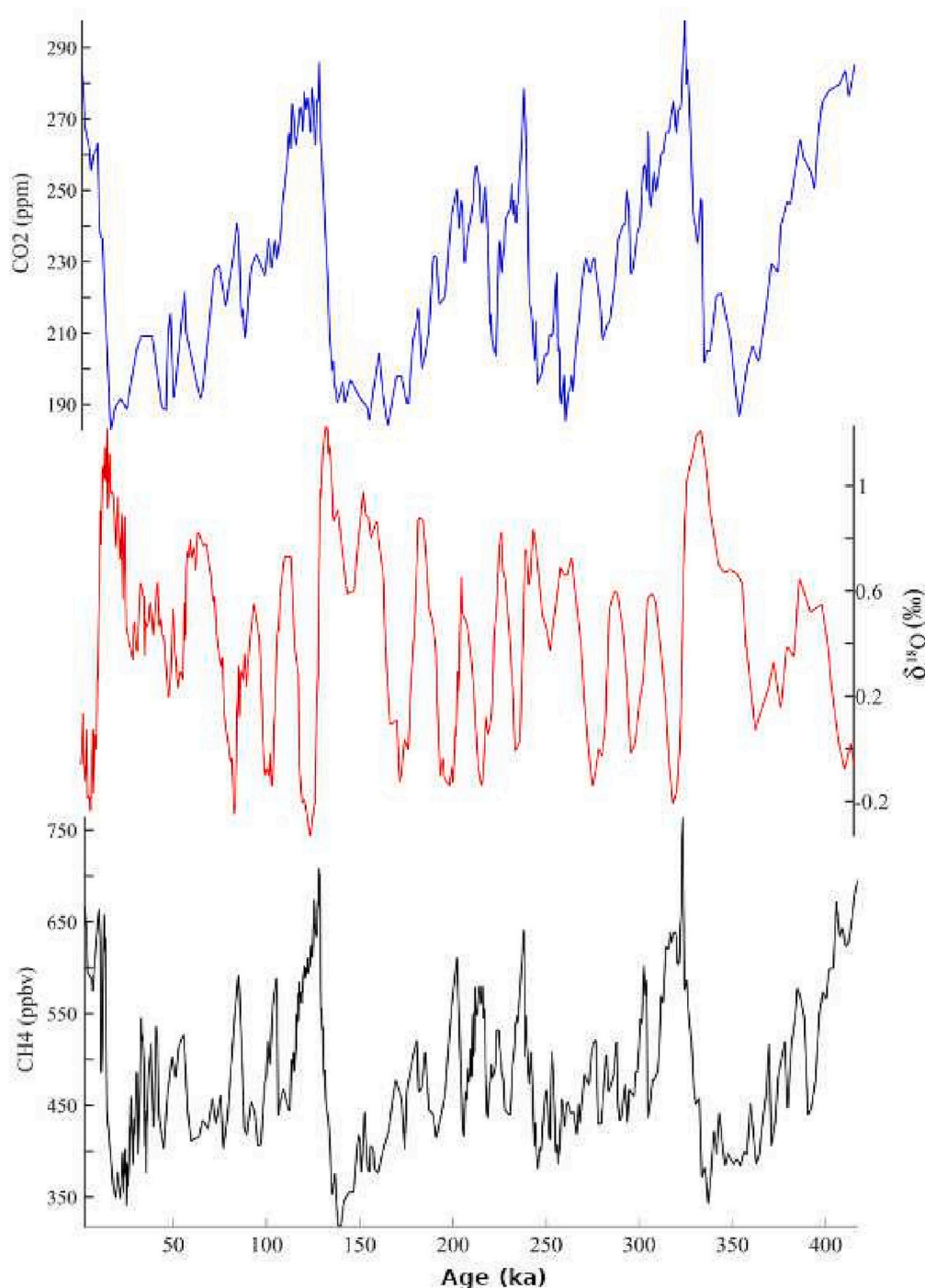


Fig. 11. Using data from the Vostok Ice Core, the upper blue curve shows the atmospheric carbon dioxide concentration. The middle red curve represents $\delta^{18}\text{O}$. The lower black curve represents the atmospheric methane concentration. All three quantities are plotted as a function of time for the last four hundred thousand years according to [Petit et al. \(1999\)](#) and [Lopes et al. \(2021\)](#).

variations in solar irradiance arriving at the Earth, but modified in part by internal feedback mechanisms. Without reference to the distribution of glacials and interglacials, [Olsen et al. \(2019\)](#) used lacustrine sediments to investigate the effects of the other planets on the fundamental frequencies of precession of the perihelion of Earth from 223 to 199 Ma. They concluded that only the frequencies produced by Jupiter were consistent with the present-day frequencies. [Hinnov \(2018\)](#) represents a significant advance, with uncertain assumptions omitted. Modern cyclostratigraphy is, of course, only possible because it has been shown that many short- and intermediate-period processes of sedimentology

are controlled by celestial mechanics of the solar system. This celestial mechanics describes approximately reversible processes. Only reversible processes can be cyclic in the physical sense. Endogenously controlled geological processes, on the other hand, which are essentially controlled by the thermal evolution of the Earth's mantle, cannot be truly cyclic for fundamental physical reasons, as shown by [Walzer and Hendel \(2022\)](#). Cyclostratigraphy is now an important tool for estimating the influence of solar irradiance variations on natural climate changes caused in part by changes in eccentricity, obliquity, and precession. [Sinnesael et al. \(2019\)](#) demonstrate this using three examples from the late Miocene,

Pleistocene, and late Devonian. These considerations were further developed by Laskar (2020). He concluded that the influences of the individual planets on the eccentricity of the Earth's orbit are very different. Larger planets change the eccentricity in a steady state manner. Smaller planets produce more random changes in eccentricity. While the motions of the minor planets Ceres and Vesta are partly chaotic, the motions of Jupiter and Saturn are almost in a steady state. For the geologically short time of the last million years (Fig. 10), the observed recent periodicity component of the eccentricity, g_2 – g_5 , of 405 ka can therefore be used for back-calculations. The incoming solar energy depends also on obliquity and precession. The dissipation of the Earth–Moon system means the corresponding solution is more complex than that of just the eccentricity. However, Laskar (2020) provided a more exact solution to this cycle, which is suitable for the back-projections. To eliminate the effect of the chaotic motion of the inner planets, Mogavero and Laskar (2021) developed a new secular dynamic model for the inner planets that is consistent with the most precise orbital solutions currently available. They used the regularity in the secular motion of the outer planets (Jupiter to Neptune) to obtain a quasi-periodic solution for the orbits of the inner planets. Given the above results, we conclude that although the Milankovitch theory is not yet firmly established, it is, in combination with some feedback mechanisms, the best hypothesis to explain the temporal distribution of glacial and interglacials in the recent ice age. Thus, most studies consider that a modified form of the Milankovitch theory is appropriate. On the other hand, the hypotheses of gradual climate evolution and of *ice ages* presented in Sections 2 and 3, apart from the rejected high-obliquity hypothesis, assume that climate evolution occurs *inside* the solid-Earth–ocean–atmosphere–biosphere system. In contrast, the *glacials and interglacials* are controlled by the *celestial mechanics* of our planetary system (Laskar et al., 2011; Rosengren and Scheeres, 2014; Laskar, 2019; Laskar, 2020), i.e., *glacials and interglacials are controlled from the outside*.

Finally, it is worth noting that there are now other papers applying Milankovitch theory to earlier, i.e. non-Pleistocene, glaciations, e.g., Benn et al. (2015), Meyers and Malinverno (2018), Lantink et al. (2019), Sørensen et al. (2020), Cheng et al. (2020), Mitchell et al. (2021).

5.2. Relatively short-term effects that influence natural climate and weather from the outside

Sections 2 and 3 have shown that the faint young Sun paradox and slow natural climate change can be explained by a decrease in atmospheric greenhouse gases, especially CO₂, due to the inorganic silicate-carbonate cycle. The occurrence of Paleoproterozoic and Cryogenic glaciations, however, is caused by LIPs in conjunction with the physical climatology at the time of eruption, the proximity of the LIPs to the paleo-equator, and other influences. We will now address some minor and short-term effects that are controlled from outside the Earth system. Earth's magnetic field extends far into space and generates the magnetosphere that has a complicated structure, which is essentially known for the present-day, i.e., in case of a dominating dipole. The solar wind deforms the magnetosphere. The outermost layer of the magnetosphere is the bow shock, which is now located 90,000 km in a sunward direction from Earth. The bow shock screens Earth from most incoming electrically charged particles of the solar wind (Lyon, 2000; Gingell et al., 2020) and galactic cosmic rays (Blasi, 2013; Matthiä et al., 2013; Tomassetti et al., 2017; Evoli et al., 2019). At present, only a minority of these particles can enter Earth's atmosphere via the polar cusps. The charged particles first penetrate the exosphere, and then the thermosphere, mesosphere, stratosphere, and, finally, troposphere. The interactions with the ions, atoms, and molecules in the upper atmospheric layers are complex, nonlinear, and turbulent. For this reason, a small energy input can generate large effects. Therefore, it is incorrect to conclude that a very small input of energy can only produce small effects. Unfortunately, this simple conclusion has been often ignored.

Fortunately, the Earth has a second protective shield, which is the heliosphere. The cubic extent of the heliosphere is determined by the heliospheric magnetic field and solar wind. The outer boundary of the heliosphere is the termination shock generated by the stellar winds from stars not far away, which stop the solar wind at this variable boundary. The slightly fluctuating 22-years solar magnetic cycle (Solanki et al., 2006) directly influences the heliosphere, and thereby the form of Earth's magnetosphere, and the number of charged cosmic ray particles reaching Earth's magnetosphere. Beer et al. (2018) showed that the same is true for other periodic processes over the last 10 000 years. The continuation of 87-years Gleissberg cycles during supermodulation events suggests that the Hale and Schwabe cycles persist irrespective of the modulation mechanism. They also studied the behavior of solar activity during the Spörer and Maunder minima. Such large minima repeat with a period of about 208 years. However, the Hallstatt cycle, with a period of about 2300 years, is also superimposed on these cycles.

The heliosphere is not spherical. Ion and Neutral Camera (INCA) line-of-sight observations (Schwadron and Bzowski, 2018) have shown its geometry varies in response to episodic cooling and heating of the inner heliosheath plasma. The solar dynamo theory has many unresolved problems (Parker, 2009). The long-term behavior of the solar dynamo is largely unknown. Even in the case of a steady-state cosmic ray flux from the outside, sudden changes from a dipolar to a weak-field state could possibly produce sudden changes in the cosmic ray flux arriving at the upper atmospheric layers of Earth. However, Laken et al. (2012) concluded that there is no clear evidence of a link between cosmic ray flux and clouds. Lockwood (2012) showed that galactic cosmic rays have virtually no effect on variations in cloud cover, especially for low-altitude clouds. Erlykin et al. (2013) concluded that cosmic rays do not significantly affect clouds, at least if H₂SO₄ is the dominant source of aerosols. These have been the main reasons for the rejection of the direct causal link between cosmic rays arriving on Earth and cloud formation in the troposphere proposed by Svensmark and Friis-Christensen (1997) and Svensmark et al. (2009). Lanci et al. (2020) compared foraminiferal $\delta^{18}\text{O}$ data, which are a proxy for paleoclimate, to magnetic paleointensity, which is a proxy for galactic cosmic ray flux, and found virtually no correlation. One must admit that the comparison was only for Pacific ODP Site 1218 and comprised only 3.6 Ma from the Oligocene.

We now discuss whether there is, for short periods of time, a robust link between natural climate change and the variability of the solar and terrestrial magnetic fields and thus indirectly also the variability of cosmic rays. We deliberately do not deal with theories but focus on a comparison of observations and, where possible, measurements. We do not connect this problem to microphysical mechanisms, as the processes in the heliosphere, terrestrial magnetosphere, and upper atmospheric layers are highly turbulent. It is clear that $\delta^{18}\text{O}$ data from foraminifera, corals, and ice cores can be used as a proxy for temperature. Some radioisotopes with short half-lives, τ , are created by the action of cosmic rays: ¹⁰Be with $\tau = 1.387$ Ma by cosmic ray spallation of nitrogen and oxygen; ¹⁴C with $\tau = 5730$ a by the ¹⁴N(n,p)¹⁴C reaction; ²⁶Al with $\tau = 717$ ka by spallation of argon; ³⁶Cl with $\tau = 301$ ka by the ³⁵Cl(n, γ)³⁶Cl reaction; ⁴¹Ca with $\tau = 99.4$ ka (Jörg et al., 2012) by the ⁴⁰Ca(n, γ)⁴¹Ca reaction; ¹²⁹I with $\tau = 15.7$ Ma by spallation of xenon.

A significant, sudden, and anomalous increase in $\Delta^{14}\text{C}$ values has been observed at A.D. 774–775 in tree rings from Japan (Miyake et al., 2012), Germany (Usoskin et al., 2013), New Zealand (Güttler et al., 2013), and Russia and America (Jull et al., 2014). Therefore, the global nature of this event is clear. All explanations for this phenomenon assume an extraterrestrial origin. Most studies have concluded that an enhanced solar proton flux caused the anomalous change in $\Delta^{14}\text{C}$ values, since there is no observational basis for more distant sources. Historical chronicles have described auroral activity. Liu et al. (2014) compared the $\Delta^{14}\text{C}$ and $\delta^{18}\text{O}$ records, and proposed a cometary impact occurred, but this hypothesis was rejected by Jull et al. (2014) and other studies.

Elevated $\Delta^{14}\text{C}$ values are associated with colder summers in the following years. Mekhaldi et al. (2015) investigated the AD 774–775 event by combining ice core and tree ring records of ^{10}Be , ^{14}C , and ^{36}Cl . They showed that peaks of these isotopes were produced by extreme solar events. The ice core ^{36}Cl in combination with ^{10}Be data show that these solar events had a very hard energy spectrum with energies >100 MeV. Uusitalo et al. (2018) demonstrated the latitudinal dependence of the ^{14}C intensity of the AD 774–775 event. A particle-induced ^{14}C poleward increase is consistent with a very large Solar Particle Event (SPE) as the real cause of the AD 774–775 terrestrial observations. The analysis of Maehara et al. (2015) showed that solar flares with energies between 10^{33} and 10^{34} erg could have produced the AD 774–775 event. Büntgen et al. (2018) investigated ^{14}C tree ring data for events in AD 774 and 993, as well as corresponding space weather, and also suggested strong solar proton radiation occurred at these times. A similar solar proton event was reported by Sakurai et al. (2020) to have occurred in 660 BC. They measured the ^{14}C abundances of early and late woods in the annual rings of a Japanese cedar tree, and discussed the possibility that consecutive SPEs occurred over three years. We emphasize that solar flares and superflares are generated by the emergence of the magnetic field from the interior of the Sun to the solar atmosphere, local augmentation of electrical currents in the Sun's corona, and rapid dissipation of electrical current. This process produces shock heating and a large ejection of charged particles (Shibata and Magara, 2011). The preceding discussion has shown that space weather and the weather in the higher atmosphere of Earth is clearly influenced by the Sun's magnetic activity, at least for short-duration events.

Now we examine longer timescales of several decades. Kirkby (2007) showed that the incoming cosmic ray intensity at stations in Murmansk, Mirny (Antarctica), and Moscow is strongly correlated with sunspot numbers, although there is a slight time lag. Low sunspot numbers correlate with low solar magnetic activity, and an enhanced galactic

cosmic ray flux is observed in the atmosphere and on Earth's surface, especially in two circular belts around the two magnetic poles of the Earth. A strong heliosphere shields Earth from most galactic cosmic rays. The cosmic ray reconstructions are mainly based on ^{14}C measurements in tree rings and ^{10}Be measurements in ice cores, but also on the other nuclides mentioned above. Similar conclusions can be drawn from Fig. 12. Kirkby (2007) showed a correlation between the temperature of the atmosphere and incoming galactic cosmic rays (Fig. 13). However, the physical mechanisms behind this correlation appear to be more complex than previously thought. Beer et al. (2012) and Usoskin (2017)

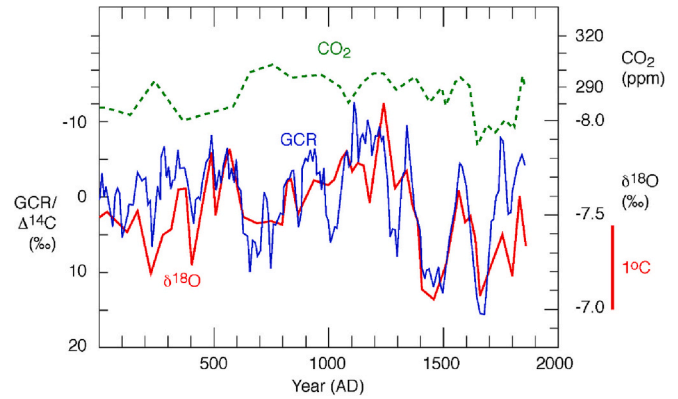


Fig. 13. Reconstruction of Alpine temperatures using $\delta^{18}\text{O}$ speleothem data from Spannagel Cave in Austria (Mangini et al., 2005) (red curve), as compared with variations in cosmic rays (blue curve) deduced from $\Delta^{14}\text{C}$ data and atmospheric CO_2 concentrations (Kirkby, 2007). This figure shows that natural climate change is strongly affected by incoming cosmic rays, at least in the European Alps, and presumably at higher geomagnetic latitudes.

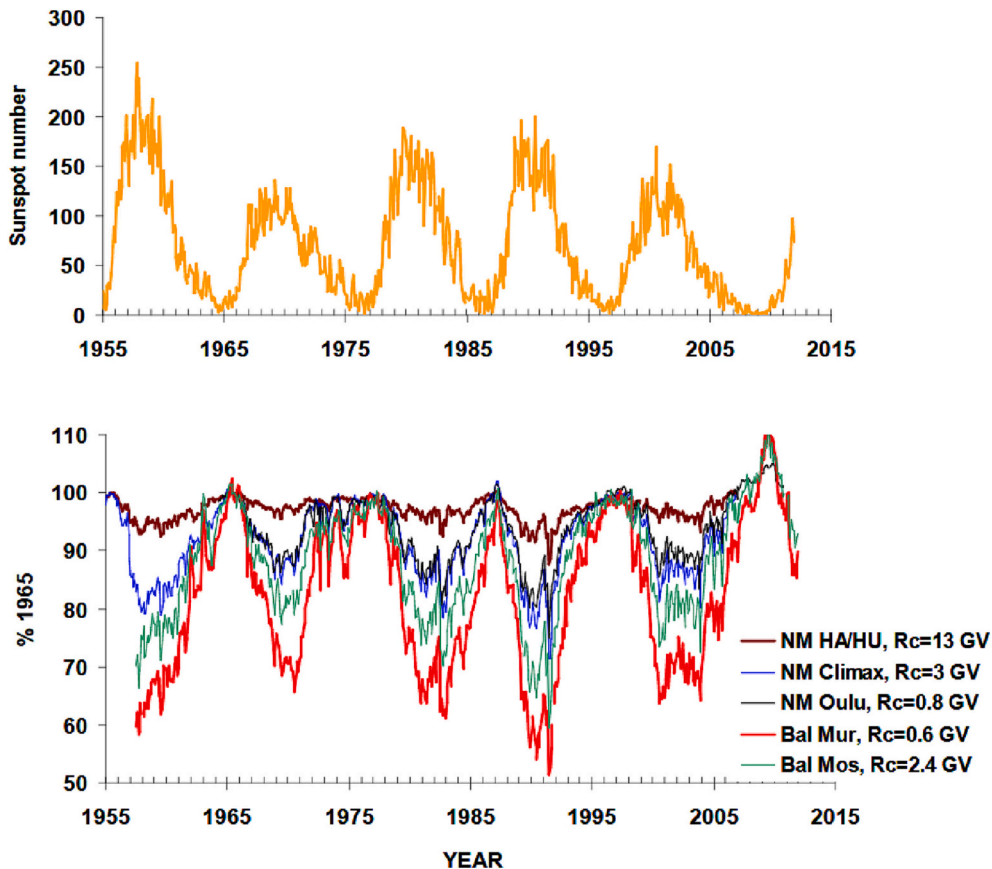


Fig. 12. Comparison of sunspot numbers (upper panel) with cosmic ray intensity (lower panel), based on Mironova et al. (2015). The cosmic ray data are normalized to 100% in 1965. Incoming cosmic rays are controlled by solar magnetic activity, because solar magnetic activity is closely related to sunspot numbers. The lower curves show that the measured cosmic ray intensity depends on the geomagnetic latitude. Furthermore, the measured cosmic ray intensity depends on the altitude of the observatory. NM = neutron monitor; Bal = balloon-carried Geiger counter. The colored curves are as follows: red = Murmansk (Mur); green = Moscow (Mos); blue = Climax; black = Oulu (Finland); brown = neutron monitors in Huancayo–Haleakala. This figure shows that a longer interruption to the solar magnetic dipole would produce an increase in incoming cosmic rays.

provide some insights into the connections between incoming galactic cosmic rays, solar and terrestrial magnetism, and natural climate change.

6. Results

(1)The impetus for this paper was our numerical model of the thermal and chemical evolution of Earth’s mantle and crust (Walzer and Hendel, 2022), in which we solved the full set of conservation equations for Earth’s history. Episodic large-scale partial melting of the asthenosphere produced precursor crustal material. *Based on our model, the growth of continental crust was episodic rather than steady state.* The global detrital zircon age distribution (Puetz and Condie, 2019; Puetz and Condie, 2022) matches our model results for the timing of crustal growth, especially if the observed peaks older than 3050 Ma have been partly removed due to potential preservation bias.

(2)The present paper focuses on the origin and temporal distribution of natural climate change and glaciations. In the Archean and Proterozoic, the faint young Sun paradox can be explained by reducing the CO₂ partial pressure by chemical weathering of silicates (i.e., Eq. (3)). Therefore, it could be expected that glaciations would occur after each peak of new juvenile continental crustal growth, but this is not the case, for both the model results and observed zircon age peaks (Fig. 1). Therefore, while the inorganic carbonate–silicate cycle is relevant to natural climate change in general, it is not sufficient to explain the timing of ice ages.

(3)An addition to the first theory is that a breakup of a supercontinent substantially increases the sum of the coastlines. This enhances the inorganic carbonate–silicate effects. If the supercontinent is located near the equator, this mechanism is again intensified, because weathering is stronger there than further poleward. Fig. 2 shows this mechanism quite well. However, it is inexplicable why this effect is not observed in the breakup of Columbia. Moreover, the Phanerozoic evolution is only remotely consistent with this idea. The observed deviations from the predictions of the mechanism of the inorganic carbonate–silicate cycle mean that another essential mechanism acts here in addition, so that the whole results from a superposition. This other essential mechanism is summarized in the next paragraph, i.e. in (4).

(4)Another theory is to assume that volcanism is essentially causing the Paleoproterozoic and Cryogenian glaciations in particular. As far as volcanism is concerned, the large igneous provinces (LIPs) prove to be particularly effective. However, this conclusion is not valid without additional assumptions. The effects of LIP eruptions from must be considered in the context of the physical climatology at the time of the outburst, the proximity of the LIPs to the paleoequator, the magnitude of the outburst, and the chemical composition of the lava and emitted gases. Several stable states in the climate system are separated by unstable jumps (bifurcations) between stable states. This is primarily a consequence of ice-albedo feedback, particularly between sea ice and the ocean. Ice-albedo feedback causes rapid advance and retraction of sea ice margins in the tropics. This explains the abrupt onset and termination of snowball Earth periods. However, it is impossible to derive the temporal boundaries of glaciations solely from LIPs because there are simply far too many LIPs. Compare Fig. 3.

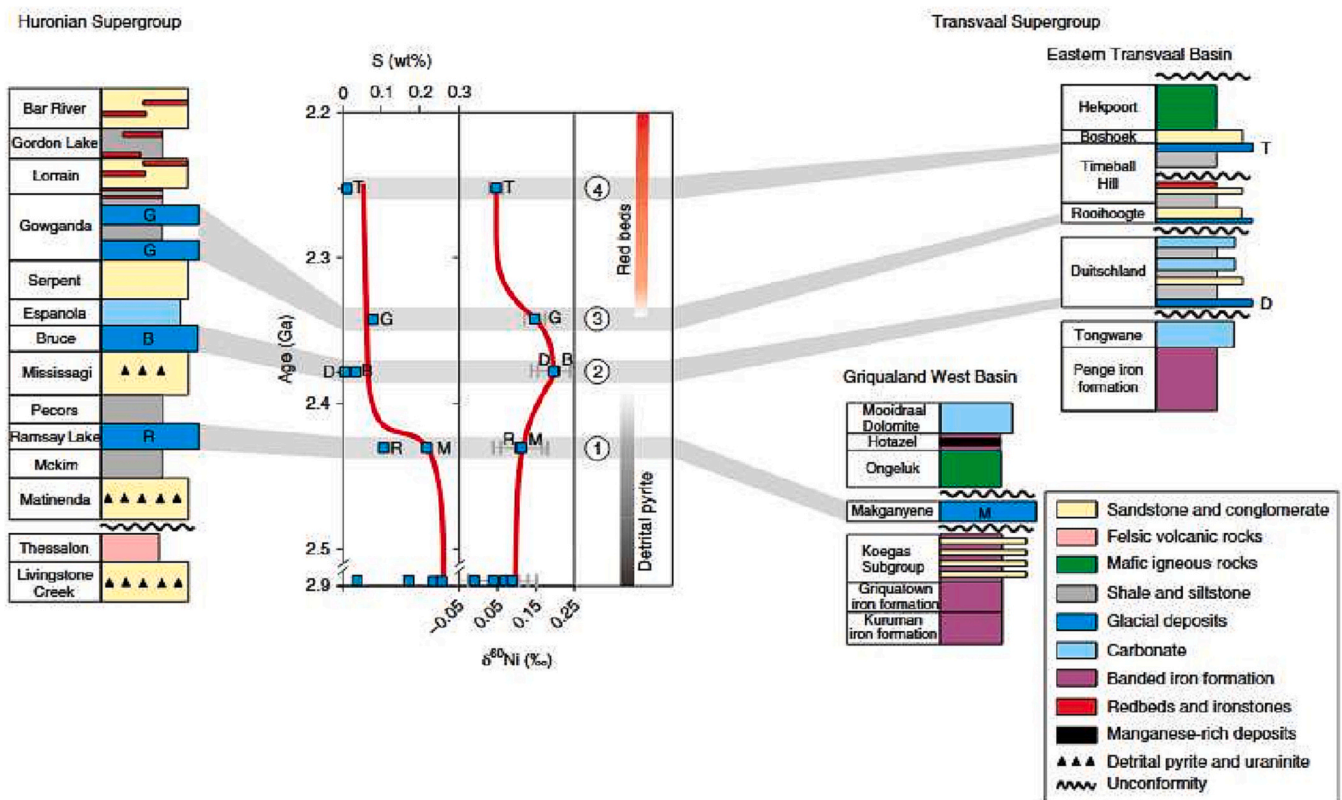


Fig. 14. Stratigraphic synthesis of the Huronian and Transvaal supergroups according to Wang et al. (2019), showing trends in total sulfur and $\delta^{60/58}\text{Ni}$ in composite diamictites. The coupled changes in total sulfur and $\delta^{60/58}\text{Ni}$ values in the four correlated glacial units with ascending stratigraphic order are consistent with geological redox indicators (that is, the disappearance of detrital pyrite and the appearance of red beds). The timings and correlations of the four glacial events are from Gumsley et al. (2017). First glaciation: Ramsay Lake (R) and Makganyene (M) formations; second glaciation: Bruce (B) and Duitschland (D) formations; third glaciation: Gowganda (G) formation; fourth glaciation: Timeball Hill (T) formation.

(5) A fourth hypothesis is that all Proterozoic ice ages occurred on Earth when the obliquity was greater than 54° and that, due to a catastrophic event after the Cryogenian, the obliquity obtained values oscillating around the present-day value between 22.1° and 24.5° . We show that it is possible to disprove this hypothesis.

(6) We show that in addition to the two main mechanisms, i.e., the inorganic carbonate–silicate cycle and the mechanism described in (4), biotic mechanisms are also at work to a lesser extent. It is suggested that the biotic influence was stronger in the Phanerozoic than before.

(7) However, the onsets and terminations of glaciations were abrupt and globally synchronous (Figs. 5 and 8). Furthermore, the number and temporal distribution of the Paleoproterozoic and Cryogenian snowball Earth epochs remain unexplained. Biotic theories cannot explain the observed temporal distribution of ice ages either (Fig. 4).

(8) Apart from the rejected hypothesis of a large obliquity change, all other hypotheses are based on the assumption that the evolution of a closed solid-Earth–hydrosphere–atmosphere–biosphere system must suffice to explain glaciations. To partially detach us from this assumption, we examined the subdivision of *one* glaciation into glacial and interglacial. We conclude that some modified form of the Milankovitch theory affected by internal feedback mechanisms is required. Therefore, the problem of glacial and interglacial is determined by the celestial mechanics of the Solar System. As such, the timing of glacial and interglacial is controlled by factors external to Earth (Fig. 10).

(9) Avoiding much debated claims on a connection between cosmic rays and tropospheric clouding, the AD 774–775 event reflects an extreme solar event and was characterized by colder summers in the subsequent period. Moreover, the incoming cosmic ray flux, as recorded by neutron monitors and balloon-carried Geiger counters and measured over several decades, shows a correlation with solar magnetic activity and average annual rainfall in the temperate zone of Earth's Northern Hemisphere (Fig. 12). For the past 2000 years, $\delta^{18}\text{O}$ values, which are a proxy for temperature, and galactic cosmic ray intensities show a close correlation, as inferred from data from an Austrian cave (Fig. 13).

(10) The very slow changes of the natural climate are due to the inorganic carbonate–silicate cycle. The major glaciations, in particular their abrupt onsets and terminations, on the other hand, can only be explained by another co-occurring mechanism outlined in (4). For the long time span between the Paleoproterozoic and the Cryogenian glaciations, an explanation has been attempted in this paper, but it must be pointed out that it may be worthwhile to search for further solutions to this problem. For mid-period climate changes, influences from outside the Earth system are detectable: The distribution of glacial and interglacial within a glaciation is controlled by the celestial mechanics of the solar system. Short-period changes are caused by changes in the magnetic field of the Sun.

Declaration of Competing Interest

The authors declare that they have no known competing financial interests or personal relationships that could have appeared to influence the work reported in this paper.

Data availability

No data was used for the research described in the article.

Acknowledgements

We thank Paul Hoffman for exceptionally numerous and very helpful suggestions for additions. We are indebted to Nasrddine Youbi for further valuable comments. We would also like to thank the editor,

Gillian Foulger, for her insightful help. We gratefully acknowledge the longstanding, confidential collaboration with John Baumgardner. We thank Dave Stegman for providing his particle code. We also thank SCC Karlsruhe and HLRS Stuttgart for the use of their supercomputing facilities. This research was partly supported by the Deutsche Forschungsgemeinschaft (Grants WA1035/5–3 and KL495/16–1).

References

- Abbot, D.S., 2014. Resolved Snowball Earth Clouds. *J. Clim.* 27, 4391–4402.
- Abbot, D.S., Voigt, A., Branson, M., Pierrehumbert, R.T., Pollard, D., Le Hir, G., Koll, D., 2012. Clouds and Snowball Earth deglaciation. *Geophys. Res. Lett.* 39.
- Abbot, D.S., Voigt, A., Li, D., Le Hir, G., Pierrehumbert, R.T., Branson, M., Pollard, D., Koll, D.D.B., 2013. Robust elements of Snowball Earth atmospheric circulation and oases for life. *J. Geophys. Res.: Atmos.* 118, 6017–6027.
- Abe-Ouchi, A., Saito, F., Kawamura, K., Raymo, M.E., Okuno, J., Takahashi, K., Blatter, H., 2013. Insolation-driven 100,000-year glacial cycles and hysteresis of ice-sheet volume. *Nature* 500, 190–193. <https://doi.org/10.1038/nature12374>.
- Anbar, A.D., Duan, Y., Lyons, T.W., Arnold, G.L., Kendall, B., Creaser, R.A., Kaufman, A. J., Gordon, G.W., Scott, C., Garvin, J., et al., 2007. A Whiff of Oxygen Before the Great Oxidation Event? *Science* 317, 1903–1906.
- Anbar, A.D., Knoll, A.H., 2002. Proterozoic Ocean Chemistry and Evolution: A Bioinorganic Bridge? *Science* 297, 1137–1142.
- Arnaut, L.G., Ibáñez, S., 2020. Self-sustained oscillations and global climate changes. *Sci. Rep.* 10 (11200), 1–18. <https://doi.org/10.1038/s41598-020-68052-9>.
- Bahcall, J.N., Pinsonneault, M.H., Basu, S., 2001. Solar models: Current epoch and time dependences, neutrinos, and helioseismological properties. *Astrophys. J.* 555, 990–1012. <https://doi.org/10.1086/321493>.
- Beer, J., McCracken, K., von Steiger, R., 2012. Cosmogenic radionuclides: Theory and applications in the terrestrial and space environments. In: *Physics of Earth and Space Environments*, vol. 26. Springer, Berlin. <https://doi.org/10.1007/978-3-642-14651-0>.
- Beer, J., Tobias, S.M., Weiss, N.O., 2018. On long-term modulation of the Sun's magnetic cycle. *Mon. Not. R. Astron. Soc.* 473, 1596–1602.
- Benn, D.I., Le Hir, G., Bao, H., Donnadiu, Y., Dumas, C., Fleming, E.J., Hambrey, M.J., McMillan, E.A., Petronis, M.S., Ramstein, G., et al., 2015. Orbitally forced ice sheet fluctuations during the Marinoan Snowball Earth glaciation. *Nat. Geosci.* 8, 704–708.
- Berger, A., 1988. Milankovitch theory and climate. *Rev. Geophys.* 26, 624–657.
- Berger, A.L., 1978. Long-term variations of daily insolation and quaternary climatic changes. *J. Atmos. Sci.* 35, 2362–2367.
- Berner, R.A., 2004. *The Phanerozoic carbon cycle: CO₂ and O₂*. Oxford University Press on Demand.
- Blasi, P., 2013. The origin of galactic cosmic rays. *Astron. Astrophys. Rev.* 21, 70. <https://doi.org/10.1007/s00159-013-0070-7>.
- Bleeker, W., 2004. Taking the pulse of planet Earth: A proposal for a new multi-disciplinary flagship project in Canadian solid Earth sciences. *Geosci. Can.* 31, 179–190.
- Braun, C., Voigt, A., Hoose, C., Ekman, A.M., Pinto, J.G., 2022. Controls on Subtropical Cloud Reflectivity during a Waterbelt Scenario for the Cryogenian Glaciations. *J. Clim.* 35, 3457–3476.
- Büntgen, U., Wacker, L., Galván, J.D., Arnold, S., Arseneault, D., Baillie, M., Beer, J., Bernabei, M., Bleicher, N., Boswijk, G., et al., 2018. Tree rings reveal globally coherent signature of cosmogenic radiocarbon events in 774 and 993 CE. *Nat. Commun.* 9 (3605), 1–7. <https://doi.org/10.1038/s41467-018-06036-0>.
- Canfield, D.E., 1998. A new model for Proterozoic ocean chemistry. *Nature* 396, 450–453.
- Caqueneau, T., Paquette, J.L., Philippot, P., 2018. U-Pb detrital zircon geochronology of the Turee Creek Group, Hamersley Basin, Western Australia: Timing and correlation of the Paleoproterozoic glaciations. *Precamb. Res.* 307, 34–50.
- Cardona, T., 2019. Thinking twice about the evolution of photosynthesis. *Open Biol.* 9, 180246.
- Cardona, T., Sánchez-Baracaldo, P., Rutherford, A.W., Larkum, A.W., 2019. Early Archean origin of Photosystem II. *Geobiology* 17, 127–150.
- Catling, D., 2014. 6.7—The Great Oxidation Event Transition. *Treatise Geochem.* 2, 177–195.
- Catling, D.C., Zahnle, K.J., 2020. The Archean atmosphere. *Sci. Adv.* 6 (eaax1420), 1–16.
- Cawood, P.A., Hawkesworth, C.J., Dhuime, B., 2013. The continental record and the generation of continental crust. *Geol. Soc. Am. Bull.* 125 (1/2), 14–32. <https://doi.org/10.1130/B30722.1>.
- Cheng, D., Zhang, S., Zhang, Z., Zhou, C., Wang, H., Yuan, X., Chen, X., 2020. An astronomically calibrated stratigraphy of the Mesoproterozoic Hongshuizhuang Formation, North China: Implications for pre-Phanerozoic changes in Milankovitch orbital parameters. *J. Asian Earth Sci.* 199 (1–11), 104408.
- Claire, M.W., Catling, D.C., Zahnle, K.J., 2006. Biogeochemical modelling of the rise in atmospheric oxygen. *Geobiology* 4, 239–269.
- Claire, M.W., Kasting, J.F., Domagal-Goldman, S.D., Stüeken, E.E., Buick, R., Meadows, V.S., 2014. Modeling the signature of sulfur mass-independent fractionation produced in the Archean atmosphere. *Geochim. Cosmochim. Acta* 141, 365–380. <https://doi.org/10.1016/j.gca.2014.06.032>. URL: <http://www.sciencedirect.com/science/article/pii/S0016703714004475>.

- Colose, C.M., Del Genio, A.D., Way, M.J., 2019. Enhanced habitability on high obliquity bodies near the outer edge of the habitable zone of Sun-like stars. *Astrophys. J.* 884 (138), 1–13. <https://doi.org/10.3847/1538-4357/ab4131>.
- Cox, G.M., Halverson, G.P., Stevenson, R.K., Vokaty, M., Poirier, A., Kunzmann, M., Li, Z. X., Denyszyn, S.W., Strauss, J.V., Macdonald, F.A., 2016. Continental flood basalt weathering as a trigger for Neoproterozoic Snowball Earth. *Earth Planet. Sci. Lett.* 446, 89–99.
- Cox, G.M., Isakson, V., Hoffman, P.F., Gernon, T.M., Schmitz, M.D., Shahin, S., Collins, A. S., Preiss, W., Blades, M.L., Mitchell, R.N., et al., 2018. South Australian U-Pb zircon (CA-ID-TIMS) age supports globally synchronous Sturtian deglaciation. *Precamb. Res.* 315, 257–263. <https://doi.org/10.1016/j.precamres.2018.07.007>.
- Crockford, P.W., Cowie, B.R., Johnston, D.T., Hoffman, P.F., Sugiyama, I., Pellerin, A., Bui, T.H., Hayles, J., Halverson, G.P., Macdonald, F.A., et al., 2016. Triple oxygen and multiple sulfur isotope constraints on the evolution of the post-Marinoan sulfur cycle. *Earth Planet. Sci. Lett.* 435, 74–83.
- Crockford, P.W., Hodgskiss, M.S., Uhlein, G.J., Caxito, F., Hayles, J.A., Halverson, G.P., 2018. Linking paleocontinents through triple oxygen isotope anomalies. *Geology* 46, 179–182.
- Crockford, P.W., Wing, B.A., Paytan, A., Hodgskiss, M.S., Mayfield, K.K., Hayles, J.A., Middleton, J.E., Ahm, A.S.C., Johnston, D.T., Caxito, F., et al., 2019. Barium-isotopic constraints on the origin of post-Marinoan barites. *Earth Planet. Sci. Lett.* 519, 234–244.
- Daines, S.J., Mills, B.J.M., Lenton, T.M., 2017. Atmospheric oxygen regulation at low Proterozoic levels by incomplete oxidative weathering of sedimentary organic carbon. *Nat. Commun.* 8, 14379. <https://doi.org/10.1038/ncomms14379>, 1–11.
- Domagal-Goldman, S.D., Meadows, V.S., Claire, M.W., Kasting, J.F., 2011. Using biogenic sulfur gases as remotely detectable biosignatures on anoxic planets. *Astrobiology* 11, 419–441. <https://doi.org/10.1089/ast.2010.0509>.
- Donnadieu, Y., Godd eris, Y., Pierrehumbert, R., Dromart, G., Fluteau, F., Jacob, R., 2006. A GEOCLIM simulation of climatic and biogeochemical consequences of Pangea breakup. *Geochem. Geophys. Geosyst.* 7 (1–21), Q11019.
- Donnadieu, Y., Godd eris, Y., Ramstein, G., N ed elec, A., Meert, J., 2004. A ‘snowball Earth’ climate triggered by continental break-up through changes in runoff. *Nature* 428, 303–306.
- Driese, S.G., Jirsa, M.A., Ren, M., Brantley, S.L., Sheldon, N.D., Parker, D., Schmitz, M., 2011. Neoproterozoic paleoweathering of tonalite and metabasalt: Implications for reconstructions of 2.69 Ga early terrestrial ecosystems and paleoatmospheric chemistry. *Precamb. Res.* 189, 1–17.
- Erlaykin, A.D., Sloan, T., Wolfendale, A.W., 2013. A review of the relevance of the ‘CLOUD’ results and other recent observations to the possible effect of cosmic rays on the terrestrial climate. *Meteorol. Atmos. Phys.* 121, 137–142. <https://doi.org/10.1007/s00703-013-0260-x>.
- Ernst, R.E., 2014. *Large Igneous Provinces*. Cambridge University Press, pp. 653.
- Ernst, R.E., Youbi, N., 2017. How Large Igneous Provinces affect global climate, sometimes cause mass extinctions, and represent natural markers in the geological record. *Palaeogeogr. Palaeoclimatol. Palaeoecol.* 478, 30–52.
- Evans, D., Beukes, N.J., Kirschvink, J.L., 1997. Low-latitude glaciation in the Palaeoproterozoic era. *Nature* 386, 262–266.
- Evans, D.A., 2006. Proterozoic low orbital obliquity and axial-dipolar geomagnetic field from evaporite palaeolatitudes. *Nature* 444, 51–55.
- Evoli, C., Aloisio, R., Blasi, P., 2019. Galactic cosmic rays after the AMS-02 observations. *Phys. Rev. D* 99 (103023), 1–14.
- Fabre, S., Berger, G., 2012. How tillite weathering during the snowball Earth aftermath induced cap carbonate deposition. *Geology* 40, 1027–1030.
- Fabre, S., Berger, G., Chavagnac, V., Besson, P., 2013. Origin of cap carbonates: An experimental approach. *Palaeogeogr. Palaeoclimatol. Palaeoecol.* 392, 524–533.
- Ferreira, D., Marshall, J., O’Gorman, P.A., Seager, S., 2014. Climate at high-obliquity. *Icarus* 243, 236–248.
- Feulner, G., 2012. The faint young Sun problem. *Rev. Geophys.* 50, RG2006. <https://doi.org/10.1029/2011RG000375>.
- Feulner, G., 2017. Formation of most of our coal brought Earth close to global glaciation. *Proc. Nat. Acad. Sci.* 114, 11333–11337.
- Feulner, G., Hallmann, C., Kienert, H., 2015. Snowball cooling after algal rise. *Nat. Geosci.* 8, 659–662.
- Foley, B.J., 2018. The dependence of planetary tectonics on mantle thermal state: applications to early Earth evolution. *Philos. Trans. R. Soc. A: Math. Phys. Eng. Sci.* 376, 20170409. <https://doi.org/10.1098/rsta.2017.0409>.
- Font, E., N ed elec, A., Trindade, R., Moreau, C., 2010. Fast or slow melting of the Marinoan snowball Earth? The cap dolostone record. *Palaeogeogr. Palaeoclimatol. Palaeoecol.* 295, 215–225.
- Gaucher, C., Frei, R., 2018. The Archean-Proterozoic Boundary and the Great Oxidation Event. Chemostratigraphy across major chronological boundaries, pp. 33–45.
- Gerya, T., 2019. Geodynamics of the early Earth: Quest for the missing paradigm. *Geology* 47, 1006–1007. <https://doi.org/10.1130/focus102019.1>.
- Gingell, I., Schwartz, S.J., Eastwood, J.P., Stawarz, J.E., Burch, J.L., Ergun, R.E., Fuselier, S.A., Gershman, D.J., Giles, B.L., Khotyaintsev, Y.V., et al., 2020. Statistics of reconnecting current sheets in the transition region of Earth’s bow shock. *J. Geophys. Res.: Space Phys.* 125, e2019JA027119.
- Godd eris, Y., Donnadieu, Y., Carretier, S., Aretz, M., Dera, G., Macouin, M., Regard, V., 2017. Onset and ending of the late Palaeozoic ice age triggered by tectonically paced rock weathering. *Nat. Geosci.* 10, 382–386.
- Godd eris, Y., Donnadieu, Y., Dessert, C., Dupr e, B., Fluteau, F., Fran ois, L.M., Meert, J., N ed elec, A., Ramstein, G., 2007. Coupled modeling of global carbon cycle and climate in the Neoproterozoic: links between Rodinia breakup and major glaciations. *C.R. Geosci.* 339 (3–4), 212–222.
- Godd eris, Y., Donnadieu, Y., Le Hir, G., Lefebvre, V., Nardin, E., 2014. The role of palaeogeography in the Phanerozoic history of atmospheric CO₂ and climate. *Earth Sci. Rev.* 128, 122–138.
- Goodman, J.C., Pierrehumbert, R.T., 2003. Glacial flow of floating marine ice in ‘Snowball Earth’. *J. Geophys. Res.: Oceans* 108.
- Goodman, J.C., Strom, D.C., 2013. Feedbacks in a coupled ice-atmosphere-dust model of the glacial Neoproterozoic ‘Mudball Earth’. *J. Geophys. Res.: Atmos.* 118, 11–546.
- Gumsley, A.P., Chamberlain, K.R., Bleeker, W., S oderlund, U., de Kock, M.O., Larsson, E. R., Bekker, A., 2017. Timing and tempo of the Great Oxidation Event. *Proc. Nat. Acad. Sci.* 114, 1811–1816.
- G uttler, D., Beer, J., Bleicher, N., Boswijk, G., Hogg, A., Palmer, J., Wacker, L., Wunder, J., 2013. The 774/775 AD event in the southern hemisphere. Annual report of the Laboratory of Ion Beam Physics, ETH Z urich, Switzerland, pp. 33.
- Halverson, G.P., Porter, S.M., Gibson, T.M., 2018. Dating the late Proterozoic stratigraphic record. *Emerg. Top. Life Sci.* 2, 137–147.
- Harland, W., 1964. Critical evidence for a great infra-Cambrian glaciation. *Geol. Rundsch.* 54, 45–61.
- Hawes, I., Jungblut, A., Matys, E., Summons, R., 2018. The ‘Dirty Ice’ of the McMurdo Ice Shelf: analogues for biological oases during the Cryogenian. *Geobiology* 16, 369–377.
- Hays, J.D., Imbrie, J., Shackleton, N.J., 1976. Variations in the Earth’s Orbit: Pacemaker of the Ice Ages: For 500,000 years, major climatic changes have followed variations in obliquity and precession. *Science* 194, 1121–1132.
- Heubeck, C., Engelhardt, J., Byerly, G.R., Zeh, A., Sell, B., Luber, T., Lowe, D.R., 2013. Timing of deposition and deformation of the Moodies Group (Barberton Greenstone Belt, South Africa): Very-high-resolution of Archean surface processes. *Precamb. Res.* 231, 236–262.
- Heubeck, C., Lowe, D.R., 1994. Depositional and tectonic setting of the Archean Moodies Group, Barberton Greenstone Belt, South Africa. *Precamb. Res.* 68, 257–290.
- Heubeck, C., Lowe, D.R., 1994. Late syndeformational deformation and detachment tectonics in the Barberton Greenstone Belt, South Africa. *Tectonics* 13 (6), 1514–1536.
- Higgins, J.A., Schrag, D.P., 2003. Aftermath of a snowball Earth. *Geochem. Geophys. Geosyst.* 4 <https://doi.org/10.1029/2002GC000403>.
- Hinnov, L.A., 2018. Cyclostratigraphy and Astrochronology in 2018. In: *Stratigraphy & Timescales*, vol. 3. Elsevier, pp. 1–80.
- Hoffman, P., 2016. Cryoconite pans on Snowball Earth: supraglacial oases for Cryogenian eukaryotes? *Geobiology* 14, 531–542.
- Hoffman, P.F., 2009. Pan-glacial—a third state in the climate system. *Geol. Today* 25, 100–107.
- Hoffman, P.F., 2013. The Great Oxidation and a Siderian snowball Earth: MIF-S based correlation of Paleoproterozoic glacial epochs. *Chem. Geol.* 362, 143–156.
- Hoffman, P.F., Abbot, D.S., Ashkenazy, Y., Benn, D.I., Brocks, J.J., Cohen, P.A., Cox, G. M., Creveling, J.R., Donnadieu, Y., Erwin, D.H., et al., 2017. Snowball Earth climate dynamics and Cryogenian geology-geobiology. *Sci. Adv.* 3 (e1600983), 1–43.
- Hoffman, P.F., Halverson, G.P., Domack, E.W., Husson, J.M., Higgins, J.A., Schrag, D.P., 2007. Are basal Ediacaran (635 Ma) post-glacial ‘cap dolostones’ diachronous? *Earth Planet. Sci. Lett.* 258, 114–131.
- Hoffman, P.F., Halverson, G.P., Schrag, D.P., Higgins, J.A., Domack, E.W., Macdonald, F. A., Pruss, S.B., Bl attler, C.L., Crockford, P.W., Hodgkin, E.B., et al., 2021. Snowballs in Africa: sectioning a long-lived Neoproterozoic carbonate platform and its bathyal foreslope (NW Namibia). *Earth Sci. Rev.* 219 (1–231), 103616.
- Hoffman, P.F., Kaufman, A.J., Halverson, G.P., Schrag, D.P., 1998. A Neoproterozoic snowball Earth. *Science* 281, 1342–1346.
- Hoffman, P.F., Li, Z.X., 2009. A palaeogeographic context for Neoproterozoic glaciation. *Palaeogeogr. Palaeoclimatol. Palaeoecol.* 277, 158–172.
- Hoffman, P.F., Schrag, D.P., 2002. The snowball Earth hypothesis: testing the limits of global change. *Terra nova* 14, 129–155.
- Holland, H.D., 2002. Volcanic gases, black smokers, and the Great Oxidation Event. *Geochim. Cosmochim. Acta* 66, 3811–3826.
- Huybers, P., 2011. Combined obliquity and precession pacing of late Pleistocene deglaciations. *Nature* 480, 229–232. <https://doi.org/10.1038/nature10626>.
- Huybers, P.J., Liautaud, P., Hodell, D.A., 2019. Identification of substantial precession variability in early-Pleistocene glacial cycles supports a continuous Milankovitch-type response to insolation forcing. *American Geophysical Union. Fall Meeting 2019*, PP22B–14.
- Imbrie, J., Imbrie, K.P., 1986. *Ice Ages: Solving the Mystery*. Harvard University Press.
- James, N.P., Narbonne, G.M., Kyser, T.K., 2001. Late Neoproterozoic cap carbonates: Mackenzie Mountains, northwestern Canada: precipitation and global glacial meltdown. *Can. J. Earth Sci.* 38, 1229–1262.
- Jellinek, A., Lenardic, A., Pierrehumbert, R., 2020. Ice, Fire, or Fizzle: The Climate Footprint of Earth’s Supercontinental Cycles. *Geochem. Geophys. Geosyst.* 21, e2019GC008464.
- Jiang, G., Kennedy, M.J., Christie-Blick, N., Wu, H., Zhang, S., 2006. Stratigraphy, sedimentary structures, and textures of the late Neoproterozoic Doushantuo cap carbonate in South China. *J. Sediment. Res.* 76, 978–995.
- J org, G., Amelin, Y., Kossert, K., von Gostomski, C.H., 2012. Precise and direct determination of the half-life of ⁴¹Ca. *Geochim. Cosmochim. Acta* 88, 51–65.
- Joshi, M.M., Mills, B.J.W., Johnson, M., 2019. A capacitor-discharge mechanism to explain the timing of orogeny-related global glaciations. *Geophys. Res. Lett.* 46, 8347–8354.
- Jull, A.T., Panyushkina, I.P., Lange, T.E., Kukarskih, V.V., Myglan, V.S., Clark, K.J., Salzer, M.W., Burr, G.S., Leavitt, S.W., 2014. Excursions in the ¹⁴C record at AD 774–775 in tree rings from Russia and America. *Geophys. Res. Lett.* 41, 3004–3010. <https://doi.org/10.1002/2014GL059874>.

- Kanzaki, Y., Murakami, T., 2015. Estimates of atmospheric CO₂ in the Neoproterozoic from paleosols. *Geochim. Cosmochim. Acta* 159, 190–219.
- Kaufmann, R.K., Juselius, K., 2016. Testing competing forms of the Milankovitch hypothesis: A multivariate approach. *Paleoceanography* 31, 286–297. <https://doi.org/10.1002/2014PA002767>.
- Kennedy, M., Droser, M., Mayer, L.M., Pevear, D., Mrofk, D., 2006. Late Precambrian Oxygenation; Inception of the Clay Mineral Factory. *Science* 311, 1446–1449.
- Kippenhahn, R., Weigert, A., Weiss, A., 2013. *Stellar Structure and Evolution*. Astronomy and Astrophysics Library ed.. Springer, Berlin. <https://doi.org/10.1007/978-3-642-30304-3>.
- Kirkby, J., 2007. Cosmic rays and climate. *Surv. Geophys.* 28, 333–375.
- Kirschvink, J.L., 1992. Late Proterozoic low-latitude global glaciation: the snowball Earth. In: Schopf, J.W., Klein, C. (Eds.), *The Proterozoic biosphere: a multidisciplinary study*. Cambridge University Press, pp. 51–52.
- Kirschvink, J.L., Gaidos, E.J., Bertani, L.E., Beukes, N.J., Gutzmer, J., Maepa, L.N., Steinberger, R.E., 2000. Paleoproterozoic snowball Earth: Extreme climatic and geochemical global change and its biological consequences. *Proc. Nat. Acad. Sci.* 97 (4), 1400–1405. <https://doi.org/10.1073/pnas.97.4.1400>.
- Knoll, A.H., 2014. Paleobiological perspectives on early eukaryotic evolution. *Cold Spring Harb. Perspect. Biol.* 6 (a016121), 1–14.
- Knoll, A.H., Javaux, E.J., Hewitt, D., Cohen, P., 2006. Eukaryotic organisms in Proterozoic oceans. *Philos. Trans. R. Soc. B: Biol. Sci.* 361, 1023–1038.
- Kopp, R.E., Kirschvink, J.L., Hilburn, I.A., Nash, C.Z., 2005. The Paleoproterozoic snowball Earth: A climate disaster triggered by the evolution of oxygenic photosynthesis. *Proc. Nat. Acad. Sci.* 102, 11131–11136.
- van Kranendonk, M.J., 2010. Two types of Archean continental crust: Plume and plate tectonics on early Earth. *Am. J. Sci.* 310, 1187–1209.
- Kump, L.R., 2008. The rise of atmospheric oxygen. *Nature* 451, 277–278.
- Laken, B.A., Pallé, E., Calogović, J., Dunne, E.M., 2012. A cosmic ray-climate link and cloud observations. *J. Space Weather Space Clim.* 2 (A18), 1–13. <https://doi.org/10.1051/swsc/2012018>.
- Lanci, L., Galeotti, S., Grimani, C., Huber, M., 2020. Evidence against a long-term control on Earth climate by Galactic Cosmic Ray Flux. *Global Planet. Change* 185 (1–7), 103095.
- Lang, X., Shen, B., Peng, Y., Xiao, S., Zhou, C., Bao, H., Kaufman, A.J., Huang, K., Crockford, P.W., Liu, Y., et al., 2018. Transient marine euxinia at the end of the terminal Cryogenian glaciation. *Nat. Commun.* 9, 3019. <https://doi.org/10.1038/s41467-018-05423-x>.
- Lantink, M.L., Davies, J.H., Mason, P.R., Schaltegger, U., Hilgen, F.J., 2019. Climate control on banded iron formations linked to orbital eccentricity. *Nat. Geosci.* 12, 369–374.
- Laskar, J., 2019. Astronomical solutions for paleoclimate studies. Historical views and new challenges. *Geophys. Res. Abstr.* 21, 1.
- Laskar, J., 2020. Astrochronology. In: *Geologic Time Scale 2020*. Elsevier, pp. 139–158. <https://doi.org/10.1016/B978-0-12-824360-2.00004-8>.
- Laskar, J., Fienga, A., Gastineau, M., Manche, H., 2011. La2010: a new orbital solution for the long-term motion of the Earth. *Astron. Astrophys.* 532 (A89), 1–15. <https://doi.org/10.1051/0004-6361/201116836>.
- Laskar, J., Joutel, F., Robutel, P., 1993. Stabilization of the Earth's obliquity by the Moon. *Nature* 361, 615–617.
- Le Hir, G., Donnadieu, Y., Goddard, Y., Pierrehumbert, R.T., Halverson, G.P., Macouin, M., Nédélec, A., Ramstein, G., 2009. The snowball Earth aftermath: Exploring the limits of continental weathering processes. *Earth Planet. Sci. Lett.* 277, 453–463.
- Li, D., Pierrehumbert, R.T., 2011. Sea glacier flow and dust transport on Snowball Earth. *Geophys. Res. Lett.* 38.
- Li, Z.X., Bogdanova, S.V., Collins, A.S., Davidson, A., De Waele, B., Ernst, R.E., Fitzsimons, I.C.W., Fuck, R.A., Gladkochub, D.P., Jacobs, J., et al., 2008. Assembly, configuration, and break-up history of Rodinia: A synthesis. *Precamb. Res.* 160, 179–210.
- Lisiecki, L.E., 2010. Links between eccentricity forcing and the 100,000-year glacial cycle. *Nat. Geosci.* 3, 349–352. <https://doi.org/10.1038/ngeo828>.
- Lisiecki, L.E., Raymo, M.E., 2005. A Pliocene-Pleistocene stack of 57 globally distributed benthic $\delta^{18}\text{O}$ records. *Paleoceanography* 20, 1–17. <https://doi.org/10.1029/2004PA001071>. PA 1003.
- Liu, W., Fedorov, A.V., Xie, S.P., Hu, S., 2020. Climate impacts of a weakened Atlantic Meridional Overturning Circulation in a warming climate. *Sci. Adv.* 6, eaaz4876.
- Liu, Y., Zhang, Z.F., Peng, Z.C., Ling, M.X., Shen, C.C., Liu, W.G., Sun, X.C., Liu, K.X., Sun, W., 2014. Mysterious abrupt carbon-14 increase in coral contributed by a comet. *Sci. Rep.* 3728, 1–4. <https://doi.org/10.1038/srep03728>.
- Lockwood, M., 2012. Solar influence on global and regional climates. *Surv. Geophys.* 33 (3–4), 503–534.
- Lopes, F., Zuddas, P., Courtillot, V., Le Mouél, J.L., Boulé, J.B., Mainault, A., Gèze, M., 2021. Milankovic Pseudo-cycles Recorded in Sediments and Ice Cores Extracted by Singular Spectrum Analysis. *Clim. Past Discuss.* 1–17 <https://doi.org/10.5194/cp-2021-126>.
- Luo, G., Ono, S., Beukes, N.J., Wang, D.T., Xie, S., Summons, R.E., 2016. Rapid oxygenation of Earth's atmosphere 2.33 billion years ago. *Sci. Adv.* 2, e1600134.
- Lyon, J.G., 2000. The solar wind-magnetosphere-ionosphere system. *Science* 288 (5473), 1987–1991.
- Lyons, T.W., Reinhard, C.T., Planavsky, N.J., 2014. The rise of oxygen in Earth's early ocean and atmosphere. *Nature* 506, 307–315.
- Macdonald, F.A., Strauss, J.V., Rose, C.V., Dudas, F.O., Schrag, D.P., 2010. Stratigraphy of the Fort Nolloth Group of Namibia and South Africa and implications for the age of Neoproterozoic iron formations. *Am. J. Sci.* 310, 862–888.
- Macdonald, F.A., Swanson-Hysell, N.L., Park, Y., Lisi, L., Jagoutz, O., 2019. Arc-continent collisions in the tropics set Earth's climate state. *Science* 364, 181–184.
- Macdonald, F.A., Wordsworth, R., 2017. Initiation of Snowball Earth with volcanic sulfur aerosol emissions. *Geophys. Res. Lett.* 44, 1938–1946.
- Maehara, H., Shibayama, T., Notsu, Y., Notsu, S., Honda, S., Nogami, D., Shibata, K., 2015. Statistical properties of superflares on solar-type stars based on 1-min cadence data. *Earth Planets Space* 67, 1–10. <https://doi.org/10.1186/s40623-015-0217-z>.
- Mangini, A., Spötl, C., Verdes, P., 2005. Reconstruction of temperature in the Central Alps during the past 2000 yr from a $\delta^{18}\text{O}$ stalagmite record. *Earth Planet. Sci. Lett.* 235, 741–751.
- Matthiä, D., Berger, T., Mrigakshi, A.I., Reitz, G., 2013. A ready-to-use galactic cosmic ray model. *Adv. Space Res.* 51, 329–338.
- McKenzie, N.R., Horton, B.K., Loomis, S.E., Stockli, D.F., Planavsky, N.J., Lee, C.T.A., 2016. Continental arc volcanism as the principal driver of icehouse-greenhouse variability. *Science* 352, 444–447.
- McMenamin, M.A., 2004. Climate, paleoecology and abrupt change during the late Proterozoic: a consideration of causes and effects. In: *The Extreme Proterozoic: Geology, Geochemistry, and Climate*. Geophysical Monograph Series, pp. 215–229.
- Mekhaldi, F., Muscheler, R., Adolphi, F., Aldahan, A., Beer, J., McConnell, J.R., Possnert, G., Sigl, M., Svensson, A., Synal, H.A., et al., 2015. Multiradionuclide evidence for the solar origin of the cosmic-ray events of AD 774/5 and 993/4. *Nat. Commun.* 6, 8611. <https://doi.org/10.1038/ncomms9611>.
- Melles, M., Brigham-Grette, J., Minyuk, P.S., Nowaczyk, N.R., Wennrich, V., DeConto, R. M., Anderson, P.M., Andreev, A.A., Coletti, A., Cook, T.L., et al., 2012. 2.8 million years of Arctic climate change from Lake El'gygytyn, NE Russia. *Science* 337, 315–320.
- Meyers, S.R., Malinverno, A., 2018. Proterozoic Milankovitch cycles and the history of the solar system. *Proc. Nat. Acad. Sci.* 115, 6363–6368.
- Milanković, M., 1920. Théorie mathématique des phénomènes thermiques produits par la radiation solaire. Gauthier-Villars.
- Milankovitch, M.K., 1941. Kanon der Erdbestrahlung und seine Anwendung auf das Eiszeitenproblem. *R. Serbian Acad. Spec. Publ.* 133, 1–633.
- Mills, B., Watson, A.J., Goldblatt, C., Boyle, R., Lenton, T.M., 2011. Timing of Neoproterozoic glaciations linked to transport-limited global weathering. *Nat. Geosci.* 4, 861–864.
- Mironova, I.A., Aplin, K.L., Arnold, F., Bazilevska, G.A., Harrison, R.G., Krivolutsky, A. A., Nicoll, K.A., Rozanov, E.V., Turunen, E., Usoskin, I.G., 2015. Energetic particle influence on the Earth's atmosphere. *Space Sci. Rev.* 194, 1–96.
- Mitchell, R.N., Gernon, T.M., Cox, G.M., Nordsvan, A.R., Kirscher, U., Xuan, C., Liu, Y., Liu, X., He, X., 2021. Orbital forcing of ice sheets during snowball Earth. *Nat. Commun.* 12, 4187.
- Miyake, F., Nagaya, K., Masuda, K., Nakamura, T., 2012. A signature of cosmic-ray increase in AD 774–775 from tree rings in Japan. *Nature* 486, 240–242.
- Mogavero, F., Laskar, J., 2021. Long-term dynamics of the solar system inner planets. arXiv preprint arXiv:2105.14976.
- Montoya, M., Griesel, A., Levermann, A., Mignot, J., Hofmann, M., Ganopolski, A., Rahmstorf, S., 2005. The Earth system model of intermediate complexity CLIMBER-3a. Part I: description and performance for present-day conditions. *Clim. Dyn.* 25, 237–263.
- Myrow, P.M., Lamb, M., Ewing, R., 2018. Rapid sea level rise in the aftermath of a Neoproterozoic snowball Earth. *Science* 360, 649–651.
- Nance, R.D., Murphy, J.B., Santosh, M., 2014. The supercontinent cycle: a retrospective essay. *Gondwana Res.* 25, 4–29.
- Nordsvan, A.R., Barham, M., Cox, G., Kirscher, U., Mitchell, R.N., 2019. Major shoreline retreat and sediment starvation following Snowball Earth. *Terra Nova* 31, 495–502.
- Nutman, A.P., 2006. Antiquity of the oceans and continents. *Elements* 2, 223–227.
- Olsen, P.E., Laskar, J., Kent, D.V., Kinney, S.T., Reynolds, D.J., Sha, J., Whiteside, J.H., 2019. Mapping Solar System chaos with the Geological Orrery. *Proc. Nat. Acad. Sci.* 116 (22), 10664–10673.
- Opdyke, B.N., Wilkinson, B.H., 1990. Paleolatitude distribution of Phanerozoic marine ooids and cements. *Palaeogeogr. Palaeoclimatol. Palaeoecol.* 78, 135–148.
- Paillard, D., 2015. Quaternary glaciations: from observations to theories. *Quatern. Sci. Rev.* 107, 11–24.
- Parker, E.N., 2009. Solar magnetism: the state of our knowledge and ignorance. *Space Sci. Rev.* 144, 15–24.
- Pavlov, A.A., Kasting, J.F., 2002. Mass-independent fractionation of sulfur isotopes in Archean sediments: strong evidence for an anoxic Archean atmosphere. *Astrobiology* 2, 27–41.
- Petit, J.R., Jouzel, J., Raynaud, D., Barkov, N.I., Barnola, J.M., Basile, I., Bender, M., Chappellaz, J., Davis, M., Delaygue, G., et al., 1999. Climate and atmospheric history of the past 420,000 years from the Vostok ice core, Antarctica. *Nature* 399 (6735), 429–436.
- Petit, J.R., Raynaud, D., Lorius, C., Jouzel, J., Delaygue, G., Barkov, N.I., Kotlyakov, V. M., revised January 2000. Historical isotopic temperature record from the Vostok ice core. Trends: A Compendium of Data on Global Change. doi:10.3334/CDIAC/cli.006.
- Pierrehumbert, R., Abbot, D., Voigt, A., Koll, D., 2011. Climate of the Neoproterozoic. *Ann. Rev. Earth Planet. Sci.* 39, 417–460.
- Pierrehumbert, R.T., 2005. Climate dynamics of a hard snowball Earth. *J. Geophys. Res.: Atmos.* 110.
- Planavsky, N.J., Bekker, A., Hofmann, A., Owens, J.D., Lyons, T.W., 2012. Sulfur record of rising and falling marine oxygen and sulfate levels during the Lomagundi event. *Proc. Nat. Acad. Sci.* 109, 18300–18305.
- Pu, J.P., Macdonald, F.A., Schmitz, M.D., Rainbird, R.H., Bleeker, W., Peak, B.A., Flowers, R.M., Hoffman, P.F., Rioux, M., Hamilton, M.A., 2022. Emplacement of the

- Franklin large igneous province and initiation of the Sturtian Snowball Earth. *Sci. Adv.* 8, eadc9430.
- Puetz, S.J., Condie, K.C., 2019. Time series analysis of mantle cycles part I: Periodicities and correlations among seven global isotopic databases. *Geosci. Front.* 10, 1305–1326. <https://doi.org/10.1016/j.gsf.2019.04.002>.
- Puetz, S.J., Condie, K.C., 2022. A review of methods used to test periodicity of natural processes with a special focus on harmonic periodicities found in global U-Pb detrital zircon age distributions. *Earth Sci. Rev.* 224 (1–35), 103885.
- Ramme, L., Marotzke, J., 2022. Climate and ocean circulation in the aftermath of a Marinoan snowball Earth. *Clim. Past* 18, 759–774.
- Ramstein, G., Godd eris, Y., Donnadieu, Y., Sepulchre, P., Fluteau, F., Zhang, Z., Zhang, R., Su, B., Jiang, D., Schuster, M., et al., 2019. Some illustrations of large tectonically driven climate changes in Earth history. *Tectonics* 38, 4454–4464.
- Rasmussen, B., Bekker, A., Fletcher, I.R., 2013. Correlation of Paleoproterozoic glaciations based on U-Pb zircon ages for tuff beds in the Transvaal and Huronian supergroups. *Earth Planet. Sci. Lett.* 382, 173–180.
- Reinhard, C.T., Planavsky, N.J., Lyons, T.W., 2013. Long-term sedimentary recycling of rare sulphur isotope anomalies. *Nature* 497, 100–103.
- Rial, J.A., Oh, J., Reischmann, E., 2013. Synchronization of the climate system to eccentricity forcing and the 100,000-year problem. *Nat. Geosci.* 6, 289–293. <https://doi.org/10.1038/ngeo1756>.
- Rooney, A.D., Strauss, J.V., Brandon, A.D., Macdonald, F.A., 2015. A Cryogenian chronology: Two long-lasting synchronous Neoproterozoic glaciations. *Geology* 43, 459–462.
- Rooney, A.D., Yang, C., Condon, D.J., Zhu, M., Macdonald, F.A., 2020. U-Pb and Re-Os geochronology tracks stratigraphic condensation in the Sturtian snowball Earth aftermath. *Geology* 48, 625–629.
- Rosengren, A.J., Scheeres, D.J., 2014. On the Milankovitch orbital elements for perturbed Keplerian motion. *Celest. Mech. Dyn. Astron.* 118, 197–220. <https://doi.org/10.1007/s10569-013-9530-7>.
- Sagan, C., Mullen, G., 1972. Earth and Mars: Evolution of atmospheres and surface temperatures. *Science* 177, 52–56.
- Sakurai, H., Tokanai, F., Miyake, F., Horiuchi, K., Masuda, K., Miyahara, H., Ohyama, M., Sakamoto, M., Mitsutani, T., Moriya, T., 2020. Prolonged production of ¹⁴C during the ~660 BCE solar proton event from Japanese tree rings. *Sci. Rep.* 10 (660), 1–7. <https://doi.org/10.1038/s41598-019-57273-2>.
- Santosh, M., Maruyama, S., Yamamoto, S., 2009. The making and breaking of supercontinents: some speculations based on superplumes, super-downwelling and the role of tectosphere. *Gondwana Res.* 15, 324–341.
- Schirmer, B.E., Guggler, M., Donoghue, P.C., 2015. Cyanobacteria and the Great Oxidation Event: evidence from genes and fossils. *Palaeontology* 58, 769–785.
- Schr oder, S., Beukes, N.J., Armstrong, R.A., 2016. Detrital zircon constraints on the tectonostratigraphy of the Paleoproterozoic Pretoria Group, South Africa. *Precamb. Res.* 278, 362–393.
- Schwadron, N., Bzowski, M., 2018. The heliosphere is not round. *Astrophys. J.* 862 (11), 1–7. <https://doi.org/10.3847/1538-4357/aacbf>.
- Shibata, K., Magara, T., 2011. Solar flares: Magnetohydrodynamic processes. *Living Rev. Sol. Phys.* 8 (6), 5–99.
- Shields, G.A., 2005. Neoproterozoic cap carbonates: a critical appraisal of existing models and the plume world hypothesis. *Terra Nova* 17, 299–310.
- Siever, R., 1992. The silica cycle in the Precambrian. *Geochim. Cosmochim. Acta* 56, 3265–3272.
- Sinnesael, M., De Vleeschouwer, D., Zeeden, C., Batenburg, S.J., Da Silva, A.C., de Winter, N.J., Dinar es-Turell, J., Drury, A.J., Gabcacorta, G., Hilgen, F.J., et al., 2019. The cyclostratigraphy intercomparison project (cip): consistency, merits and pitfalls. *Earth Sci. Rev.* 199 (1–16), 102965.
- Solanki, S.K., Inhester, B., Schussler, M., 2006. The solar magnetic field. *Rep. Prog. Phys.* 69, 563–668.
- Sorensen, A.L., Nielsen, A.T., Thibault, N., Zhao, Z., Schovsbo, N.H., Dahl, T.W., 2020. Astronomically forced climate change in the late Cambrian. *Earth Planet. Sci. Lett.* 548 (1–13), 116475.
- Stern, R.J., Miller, N.R., 2019. Neoproterozoic glaciation—snowball Earth Hypothesis. *Encyclopedia of Geology*, second ed., pp. 1–11, doi:<https://doi.org/10.1016/B978-0-12-409548-9.12197-4>.
- Strunk, A., Knudsen, M.F., Egholm, D.L., Jansen, J.D., Levy, L.B., Jacobsen, B.H., Larsen, N.K., 2017. One million years of glaciation and denudation history in West Greenland. *Nat. Commun.* 8 (14199), 1–8. <https://doi.org/10.1038/ncomms14199>.
- Svensmark, H., Bondo, T., Svensmark, J., 2009. Cosmic ray decreases affect atmospheric aerosols and clouds. *Geophys. Res. Lett.* 36 (15) <https://doi.org/10.1029/2009GL038429>.
- Svensmark, H., Friis-Christensen, E., 1997. Variation of cosmic ray flux and global cloud coverage—a missing link in solar-climate relationships. *J. Atmos. Solar Terr. Phys.* 59 (11), 1225–1232.
- Sverjensky, D.A., Lee, N., 2010. The Great Oxidation Event and Mineral Diversification. *Elements* 6, 31–36.
- Tang, H., Chen, Y., 2013. Global glaciations and atmospheric change at ca. 2.3 Ga. *Geosci. Front.* 4, 583–596.
- Tomassetti, N., Orcinha, M., Bar o, F., Bertucci, B., 2017. Evidence for a time lag in solar modulation of galactic cosmic rays. *Astrophys. J. Lett.* 849 (L32), 1–6.
- Tosca, N.J., Johnston, D.T., Mushegian, A., Rothman, D.H., Summons, R.E., Knoll, A.H., 2010. Clay mineralogy, organic carbon burial, and redox evolution in Proterozoic oceans. *Geochim. Cosmochim. Acta* 74, 1579–1592.
- Tziperman, E., Abbot, D.S., Ashkenazy, Y., Gildor, H., Pollard, D., Schoof, C.G., Schrag, D.P., 2012. Continental constriction and oceanic ice-cover thickness in a Snowball-Earth scenario. *J. Geophys. Res.: Oceans* 117.
- Ueno, Y., Johnson, M.S., Danielache, S.O., Eskebjerg, C., Pandey, A., Yoshida, N., 2009. Geological sulfur isotopes indicate elevated OCS in the Archean atmosphere, solving faint young Sun paradox. *PNAS* 106 (35), 14784–14789. <https://doi.org/10.1073/pnas.0903518106>.
- Usoskin, I.G., 2017. A history of solar activity over millennia. *Living Rev. Sol. Phys.* 14 (3), 1–97.
- Usoskin, I.G., Kromer, B., Ludlow, F., Beer, J., Friedrich, M., Kovaltsov, G.A., Solanki, S. K., Wacker, L., 2013. The AD775 cosmic event revisited: the Sun is to blame. *Astron. Astrophys.* 552 (L3), 1–4. <https://doi.org/10.1051/0004-6361/201321080>.
- Usitalo, J., Arppe, L., Hackman, T., Helama, S., Kovaltsov, G., Miilik inen, K., M akinen, H., N ojd, P., Palonen, V., Usoskin, I., et al., 2018. Solar superstorm of AD 774 recorded subannually by Arctic tree rings. *Nat. Commun.* 9 (3495), 1–8. <https://doi.org/10.1038/s41467-018-05883-1>.
- Valley, J.W., Peck, W.H., King, E.M., Wilde, S.A., 2002. A cool early Earth. *Geology* 30, 351–354.
- Vincent, C., Fischer, A., Mayer, C., Bauder, A., Galos, S.P., Funk, M., Thibert, E., Six, D., Braun, L., Huss, M., 2017. Common climatic signal from glaciers in the European Alps over the last 50 years. *Geophys. Res. Lett.* 44, 1376–1383.
- Vincent, W., Gibson, J., Pienitz, R., Villeneuve, V., Broady, P., Hamilton, P., Howard-Williams, C., 2000. Ice Shelf Microbial Ecosystems in the High Arctic and Implications for Life on Snowball Earth. *Naturwissenschaften* 87, 137–141.
- Vincent, W.F., Mueller, D.R., Bonilla, S., 2004. Ecosystems on ice: the microbial ecology of Markham Ice Shelf in the high Arctic. *Cryobiology* 48, 103–112.
- Voice, P.J., Kowalewski, M., Eriksson, K.A., 2011. Quantifying the timing and rate of crustal evolution: global compilation of radiometrically Dated Detrital Zircon grains. *J. Geol.* 119, 109–126.
- Voigt, A., 2013. The dynamics of the Snowball Earth Hadley circulation for off-equatorial and seasonally varying insolation. *Earth Syst. Dyn.* 4, 425–438.
- Walker, J.C., Hays, P., Kasting, J.F., 1981. A negative feedback mechanism for the long-term stabilization of Earth's surface temperature. *J. Geophys. Res.: Oceans* 86, 9776–9782.
- Walzer, U., Hendel, R., 2022. Mantle evolution and continental growth events. *Earth Sci. Rev.* 232 (1–11), 104130.
- Walzer, U., Hendel, R., Baumgardner, J., 2004. The effects of a variation of the radial viscosity profile on mantle evolution. *Tectonophysics* 384, 55–90.
- Walzer, U., Hendel, R., Baumgardner, J., 2006. Plateness of the oceanic lithosphere and the thermal evolution of the Earth's mantle. In: Nagel, W.E., J ager, W., Resch, M. (Eds.), *High Performance Computing in Science and Engineering '05*. Springer, Berlin, pp. 289–304.
- Wan, S., Clift, P.D., Zhao, D., Hovius, N., Munhoven, G., France-Lanord, C., Wang, Y., Xiong, Z., Huang, J., Yu, Z., et al., 2017. Enhanced silicate weathering of tropical shelf sediments exposed during glacial lowstands: A sink for atmospheric CO₂. *Geochim. Cosmochim. Acta* 200, 123–144.
- Wang, P., Du, Y., Yu, W., Algeo, T.J., Zhou, Q., Xu, Y., Qi, L., Yuan, L., Pan, W., 2020. The chemical index of alteration (CIA) as a proxy for climate change during glacial-interglacial transitions in Earth history. *Earth Sci. Rev.* 201 (1–22), 103032.
- Wang, S.J., Rudnick, R.L., Gaschnig, R.M., Wang, H., Wasylenski, L.E., 2019. Methanogenesis sustained by sulfide weathering during the Great Oxidation Event. *Nat. Geosci.* 12, 296–300.
- Warke, M.R., Di Rocco, T., Zerkle, A.L., Lepland, A., Prave, A.R., Martin, A.P., Ueno, Y., Condon, D.J., Claire, M.W., 2020. The Great Oxidation Event preceded a Paleoproterozoic “snowball Earth”. *Proc. Nat. Acad. Sci.* 117 (24), 13314–13320.
- Warren, S.G., Brandt, R.E., Grenfell, T.C., McKay, C.P., 2002. Snowball Earth: Ice thickness on the tropical ocean. *J. Geophys. Res.: Oceans* 107, 31–1.
- Wegener, A., 1912. Die Entstehung der Kontinente. *Geol. Rundsch.* 3, 276–292.
- Wegener, A., 1920. Die Entstehung der Kontinente und Ozeane. Verlag Vieweg und Sohn, pp. 1–133.
- West, A.J., Galy, A., Bickle, M., 2005. Tectonic and climatic controls on silicate weathering. *Earth Planet. Sci. Lett.* 235, 211–228.
- Williams, G., 1975. Late Precambrian glacial climate and the Earth's obliquity. *Geol. Mag.* 112, 441–465.
- Williams, G.E., Schmidt, P.W., Young, G.M., 2016. Strongly seasonal Proterozoic glacial climate in low palaeolatitudes: Radically different climate system on the pre-Ediacaran Earth. *Geosci. Front.* 7, 555–571.
- Yang, J., Jansen, M.F., Macdonald, F.A., Abbot, D.S., 2017. Persistence of a freshwater surface ocean after a snowball Earth. *Geology* 45, 615–618.
- Yoshida, M., Santosh, M., 2011. Supercontinents, mantle dynamics and plate tectonics: A perspective based on conceptual vs. numerical models. *Earth-Sci. Rev.* 105, 1–24.
- Youbi, N., Ernst, R.E., Mitchell, R.N., Boumehdi, M.A., El Moume, W., Lahna, A.A., Bensalah, M.K., S oderlund, U., Doblas, M., Tassinari, C.C., 2021. Preliminary appraisal of a correlation between glaciations and large igneous provinces over the past 720 million years. Large Igneous Provinces: A Driver of Global Environmental and Biotic Changes, pp. 169–190.
- Youbi, N., Ernst, R.E., S oderlund, U., Boumehdi, M.A., Lahna, A.A., Tassinari, C.C.G., El Moume, W., Bensalah, M.K., 2020. The Central Iapetus magmatic province: An updated review and link with the ca. 580 Ma Gaskiers glaciation.
- Young, G.M., 2013. Precambrian supercontinents, glaciations, atmospheric oxygenation, metazoan evolution and an impact that may have changed the second half of Earth history. *Geosci. Front.* 4, 247–261.
- Young, G.M., 2018. Precambrian glacial deposits: Their origin, tectonic setting, and key role in Earth evolution. In: *Past Glacial Environments*. Elsevier, pp. 17–45. <https://doi.org/10.1016/B978-0-08-100524-8.00001-4>.

- Young, G.M., 2019. Aspects of the Archean-Proterozoic transition: How the great Huronian Glacial Event was initiated by rift-related uplift and terminated at the rift-drift transition during break-up of Lauroscandia. *Earth Sci. Rev.* 190, 171–189.
- Yu, W., Algeo, T.J., Zhou, Q., Du, Y., Wang, P., 2020. Cryogenian cap carbonate models: A review and critical assessment. *Palaeogeogr. Palaeoclimatol. Palaeoecol.* 552 (1–26), 109727.
- Zhou, C., Huyskens, M.H., Lang, X., Xiao, S., Yin, Q.Z., 2019. Calibrating the terminations of Cryogenian global glaciations. *Geology* 47, 251–254.